SAND2020-3375C

Introduction to Airborne Ground-Moving Target Indicator (GMTI) Radar

MSS Tri-Service Radar Symposium
26 June 2020
Monterey, California, USA

Dr. Armin Doerry

Detailed contact information at www.doerry.us

Unclassified – Unlimited Release

1

1

Major Sections

- **Introduction**
  - **Electromagnetic Roots**
- **GMTI Basic Processing**
- **GMTI Performance Limits**
- **GMTI Clutter Cancellation**
- **GMTI Ancillary Topics**

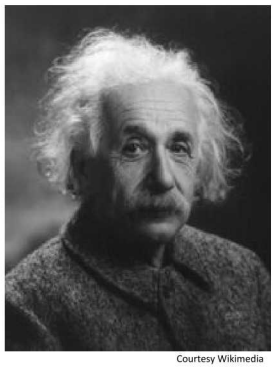

Courtesy Wikimedia

"Nothing happens until something moves."
— Albert Einstein

2

2

Brief History

- **Late 19th century**
  - **Heinrich Hertz shows radio waves can be reflected by metal objects**
- **November 1903**
  - **Christian Hülsmeyer invents "Telemobiloscope" to detect passing ships**
    - Reichspatent Nr. 165546, initially filed 21 November 1903.
- **February 1935**
  - **Robert Watson-Watt, Arnold F. 'Skip' Wilkins, conduct Daventry Experiment**
    - detected aircraft using Doppler beat signals
    - Led to Chain-Home radar system
- **Late 1950's**
  - **Concept of MTI radar for ground-movers was developed**
    - Willow Run Laboratories of the University of Michigan
    - PEEK radar
- **Late 1968**
  - **Concept developed for mounting a rotating APS-94 SLAR on a UH-1 helicopter**
    - To operate as a GMTI radar
    - Led to project ALARM
- **January 1991**
  - **two prototype Joint Surveillance Target Attack Radar System (Joint-STARS) aircraft were deployed to the Gulf**

3

3

Maxwell's Equations

Maxwell's equations relate electric fields and magnetic fields. They underpin all electrical, optical, and radio technologies.

Let there be light.

$\nabla \cdot \boldsymbol{D} = \rho$	(1) Gauss' Law
$\nabla \cdot \boldsymbol{B} = 0$	(2) Gauss' Law for magnetism
$\nabla \times \boldsymbol{E} = -\frac{\partial \boldsymbol{B}}{\partial t}$	(3) Faraday's Law
$\nabla \times \boldsymbol{H} = \frac{\partial \boldsymbol{D}}{\partial t} + \boldsymbol{J}$	(4) Ampere-Maxwell Law

$\boldsymbol{E}$ = Electric Field
$\boldsymbol{H}$ = Magnetic Field
ρ = charge density
$\boldsymbol{J}$ = current density
ε = permittivity
μ = permeability

$\boldsymbol{D} = \varepsilon \boldsymbol{E}$ = Electric Displacement field
$\boldsymbol{B} = \mu \boldsymbol{H}$ = Magnetic Induction field

Everything starts here.

4

4

Free-Space Propagation

In free-space there are no currents or charges, and no losses.

Maxwell's equations can be manipulated to

$$\nabla \times \nabla \times \boldsymbol{E} = -\mu\varepsilon \frac{\partial^2 \boldsymbol{E}}{\partial t^2}$$

and in turn, using some identities, to

$$\nabla^2 \boldsymbol{E} = \mu\varepsilon \frac{\partial^2 \boldsymbol{E}}{\partial t^2}$$

Similarly, for the magnetic field

$$\nabla^2 \boldsymbol{H} = \mu\varepsilon \frac{\partial^2 \boldsymbol{H}}{\partial t^2}$$

In Cartesian coordinates, each component of the vectors $\boldsymbol{E}$ and $\boldsymbol{H}$ satisfy a scalar wave equation.

We further identify

$$c = \frac{1}{\sqrt{\mu\varepsilon}} = \text{Propagation velocity}$$

$$\eta = \sqrt{\frac{\mu}{\varepsilon}} = \text{Characteristic wave impedance}$$

In free-space

$$\varepsilon = \varepsilon_0 \approx 8.854 \times 10^{-12} \quad \text{F/m}$$
$$\mu = \mu_0 = 4\pi \times 10^{-7} \quad \text{H/m}$$
$$c = c_0 = 299,792,458 \quad \text{m/s}$$
$$\eta = \eta_0 \approx 377 \quad \text{ohms}$$

Note that these are second-order differential equations, with solutions that are sinusoids.

5

5

Sinusoidal Plane-Wave Propagation

If traveling in the direction of the z-axis, with an electric field oriented parallel to the x-axis, our field reduces to simply

$$\boldsymbol{E} = E_x \hat{\mathbf{x}}$$

with

$\hat{\mathbf{k}} = \hat{\mathbf{z}}$ = direction of travel

$\hat{\boldsymbol{E}}_0 = \hat{\mathbf{x}}$ = field orientation

and the field equation reduces to

$$\frac{\partial^2}{\partial z^2} E_x = \frac{1}{c_0^2} \frac{\partial^2}{\partial t^2} E_x$$

with a solution

$$E_x^+(t,z) = e_1 \cos(\omega t - kz)$$

Forward/right travelling

and another solution

$$E_x^-(t,z) = e_2 \cos(\omega t + kx)$$

Backward/left travelling

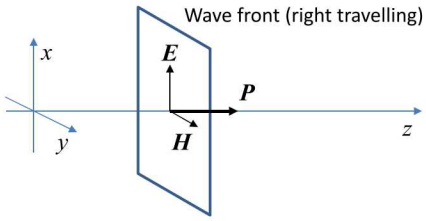

$\boldsymbol{E}$ and $\boldsymbol{H}$ fields are related as

$$\hat{\mathbf{z}} \times \boldsymbol{E} = \eta \boldsymbol{H}$$

$$\hat{\mathbf{z}} \times \boldsymbol{H} = -\frac{1}{\eta} \boldsymbol{E}$$

6

6

Plane-Wave Reflection from Perfect Conductor

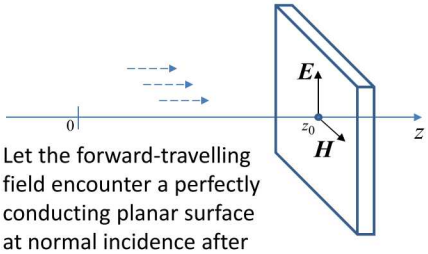

Let the forward-travelling field encounter a perfectly conducting planar surface at normal incidence after distance z_0.

At distance z_0 the forward-travelling wavefront will have travelled a time

$$t_0 = \frac{z_0}{c}$$

Recall that at the conductor surface, the tangential electric field must be zero, and the normal magnetic field must also be zero.

Boundary Conditions

For these boundary conditions to be met, we must also have generated at the surface a backward travelling wave such that

$$E_x^+(t_0, z_0) + E_x^-(t_0, z_0) = 0$$

This backward travelling field will take an additional time t_0 to reach the forward wave starting point $z = 0$

Consequently, the backward travelling field is related to the forward-travelling field by

$$E_x^-\left(2\frac{z_0}{c_0}, 0\right) = -E_x^+(0,0)$$

$$E_x^-(t,0) = -E_x^+\left(t - 2\frac{z_0}{c_0}, 0\right)$$

Radar Echo

7

Plane-Wave Reflection from Perfect Conductor

We observe that the incident and reflected fields are

$$E_x^+(t,z) = e_1 \cos(\omega t - kz)$$
$$E_x^-(t,z) = -e_1 \cos(\omega t + kz - 2kz_0)$$
$$z < z_0$$

Note that the ratio of the magnitudes of these fields is constant (unity), and independent of frequency.

Furthermore, the field equation is linear, meaning that any signal that can be written as the sum of sinusoids will exhibit the same reflection characteristics,

which means pretty much any signal we can realistically create.

These observations combine to yield the following:

A fundamental tenet of monostatic radar is that any generated/transmitted field in free-space that encounters a reflecting boundary will echo a faithful reproduction (in shape) of the incident signal, to arrive at its origin with a round-trip time delay of

$$t_{delay} = 2\frac{z_0}{c}$$ In free-space

True for all frequencies.

8

Basic Moving Target Detection (MTI) Modes

- Ground-Moving-Target Indicator (GMTI) Radar
  - GMTI Wide-Area Search (GWAS)
  - Surface-Moving-Target Indicator (SMTI)
  - Dismount Moving-Target Indicator (DMTI)
- Airborne Moving-Target Indicator (AMTI)
  - Look-down capability
- Video-SAR

9

9

Select References

- Performance Limits for Exo-Clutter Ground Moving Target Indicator (GMTI) Radar
  - Sandia National Laboratories Report SAND2010-5844
- The Standoff Observation of Enemy Ground Forces from Project Peek to JointSTARS
  - Charles A. Fowler, IEEE AES Systems Magazine, June 1997

10

10

GMTI Basic Processing

- **Basic range-velocity processing**
- **Keystone processing**
- **Range-velocity map**
- **Clutter**

- **Detection theory**
- **False alarms**
- **CFAR, CA-CFAR**
- **Detection Decisions**
- **Velocity Measure**

Basic Concepts

One radar pulse can measure time delay to a target point

Because we know the speed of the radar wave, we can calculate a target point range from that time delay.

So… with a single radar pulse we can measure **Range**

If we collect two or more radar pulses, we can measure range changes from pulse to pulse.

So… with multiple pulses we can measure **Range Rate**

Range-rate will cause a proportional Doppler shift to the radar echo.

GMTI Geometry

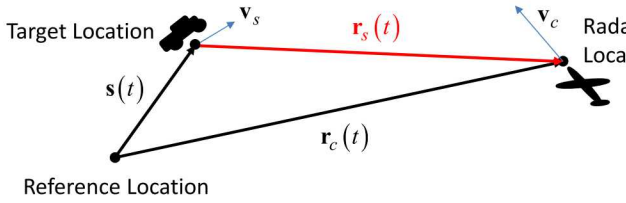

The radar will emit and collect pulses over a collection interval.

$$\mathbf{r}_c(t) = \mathbf{r}_{c,ref} + \mathbf{v}_c\left(t - t_{ref}\right)$$
$$\mathbf{s}(t) = \mathbf{s}_{ref} + \mathbf{v}_s\left(t - t_{ref}\right)$$

A radar measures range, $r_s = \left|\mathbf{r}_s(t)\right|$

Radar motion measurement subsystem can measure radar position and velocity

Target position and velocity are unknown

Our task is to detect, locate, and characterize a moving target.

The first step is to "focus" target echoes to a range-velocity map; to maximize the Signal-to-Noise Ratio (SNR) of the target echo energy.

13

13

GMTI Geometry

We can write the measured range as $r_s(t) = r_{s,ref} + v_r\left(t - t_{ref}\right)$

These components relate to the geometry vectors as

$$r_{s,ref} = \left|\mathbf{r}_s(t)\right|_{t=t_{ref}}$$
$$v_r = \mathbf{v}_r \bullet \mathbf{n}_s(t)$$

Unit vector pointing from target to radar

Depends on target and radar positions

Key observation: The range-rate (velocity) of radar from target depends on both velocity and position, of both target and radar.

Implications:

1. If the radar measures velocity, it will be the combined velocity of radar and target.
2. Only target velocities in the direction of the radar are measurable.
3. Even non-moving (stationary) targets can exhibit a velocity. This means that there is some ambiguity between target location and target velocity.

14

14

Signal Model - Transmitted

We will assume a pulse-Doppler radar, with a rectangular envelope.

The Transmitted (TX) signal for pulse number n is modelled as

$$x_T(t,n) = A_T \,\mathrm{rect}\left(\frac{t-t_n}{T}\right)\cos\left(\omega_T(t-t_n)+\Phi(t-t_n)\right)$$

time

Pulse number

Envelope

pulsewidth

Center frequency

Phase modulation

The phase modulation has bandwidth that is small compared to the center frequency. The modulation allows for range resolution via pulse compression. This could be a chirp, phase-coding, etc.

15

15

Signal Model – Received Echo

This is one of the most fundamental presumptions in radar, and the real starting point for algorithms.

The received (RX) echo signal from the target scatterer is simply an attenuated and delayed version of the transmitted signal, namely

$$x_R(t,n) = A_r \,\mathrm{rect}\left(\frac{t-t_n-\frac{2}{c}r_s(t)}{T}\right)\cos\left(\omega_T\left(t-t_n-\frac{2}{c}r_s(t)\right)+\Phi\left(t-t_n-\frac{2}{c}r_s(t)\right)\right)$$

Received amplitude

Intra-pulse Doppler scaling – assumed inconsequential

Pulse-to-pulse phase shift

This can be expanded to

$$x_R(t,n) = A_r \,\mathrm{rect}\left(\frac{t-t_n-\frac{2}{c}r_s(t)}{T}\right)\cos\left(\begin{array}{l}\omega_T\left(\left(1-\frac{2}{c}v_r\right)(t-t_n)-\frac{2}{c}r_{s,ref}-\frac{2}{c}v_r\left(t_n-t_{ref}\right)\right)\\ +\Phi\left(\left(1-\frac{2}{c}v_r\right)(t-t_n)-\frac{2}{c}r_{s,ref}-\frac{2}{c}v_r\left(t_n-t_{ref}\right)\right)\end{array}\right)$$

Modulation responsible for range response

16

16

GMTI Processing – Optimal Filtering

An optimal filter in the Mean-Squared sense is the "matched filter," or "correlator."

We implement this by creating a template for some range-velocity pair of interest, with unity amplitude, where

$$h\left(t,n,\hat{r}_{s,ref},\hat{v}_r\right) = x_R\left(t,n\right)\Big|_{\substack{A_r=1 \\ r_{s,ref}=\hat{r}_{s,ref} \\ v_r=\hat{v}_r}}$$

Then we correlate the received echo signal against this template, or kernel

$$y\left(\hat{r}_{s,ref},\hat{v}_r\right) = \sum_n \int_t x_R\left(t,n\right) h^*\left(t,n,\hat{r}_{s,ref},\hat{v}_r\right) dt$$

Very computationally expensive

where "*" denotes complex conjugate. Note that we do this for all pulses and over the entire pulse for each pulse.

Doing so for an array of interesting/desired ranges and velocities will yield a map of range-velocity responses.

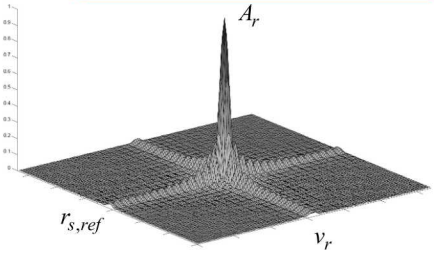

17

17

Signal Model – Range-compressed Baseband

Typical assumptions

1. Pulses collected over a Coherent Processing Interval (CPI) limited to some fraction of a second
2. Target displacement over a CPI due to its own velocity is less than the range resolution *** (will address later)
3. Relatively low velocities such that intra-pulse Doppler is inconsequential

If we violate any of these, the processing gets more complicated.

The resulting range-compressed signal may then be described as

$$x_V\left(\hat{r}_{s,ref},n\right) \approx A_r W_r\left(\frac{r_{s,ref}-\hat{r}_{s,ref}}{\rho_r}\right) \exp j\left(-\frac{2\omega_T}{c} r_{s,ref} - \frac{2\omega_T}{c} v_r\left(t_n - t_{ref}\right)\right)$$

Range resolution

Range Impulse Response (IPR)

Inconsequential constant phase

Pulse-to-pulse phase shift

This is what we customarily refer to as the "Doppler" term

18

18

GMTI Processing - Simple

Ignoring inconsequential phase terms, and performing a Discrete Fourier Transform (DFT) across pulses yields the range-velocity map

$$x_V\left(\hat{r}_{s,ref},\hat{v}_r\right) \approx A_r W_r\left(\frac{r_{s,ref}-\hat{r}_{s,ref}}{\rho_r}\right) W_v\left(\frac{v_r-\hat{v}_r}{\rho_v}\right)$$

Velocity IPR

Velocity resolution

This is a complete 2D map of range vs. velocity for a point reflector.

It peaks at $\left(r_{s,ref}, v_r\right)$

Recall that "Doppler" is proportional to velocity. Consequently, in GMTI these are often used interchangeably.

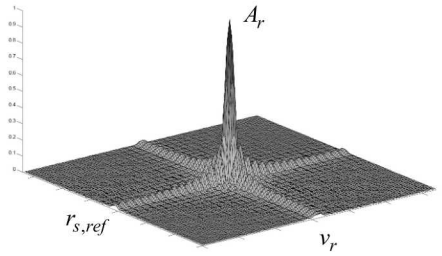

19

19

What is Doppler in GMTI Radar?

A tacit assumption in typical GMTI is that t_n increases linearly with pulse index n, i.e. constant PRF.

For GMTI, it is all about "when" the radar echoes are collected.

The "where" does affect the data, but can be mitigated with processing.

Velocity processing is often called Doppler processing. Doppler processing is typically about observing manifestations in 'slow-time'

Doppler effects within a single pulse's echo are typically ignored.

The Doppler effect (or Doppler shift) is the change in frequency of a wave (or other periodic event) for an observer moving relative to its source. It is named after the Austrian physicist Christian Doppler, who proposed it in 1842 in Prague. It is commonly heard when a vehicle sounding a siren or horn approaches, passes, and recedes from an observer.
– Wikipedia, 21 September 2017

20

20

GMTI Processing – Resolution

The question is now "If the target response is indeed an impulse, how well can we localize the target's response?"

The overall function is called the "Impulse Response" (IPR) of the GMTI range-velocity map.

The IPR width is its resolution. This is most often characterized in cardinal directions of 'range' and 'velocity'. Neglecting any sidelobe filtering, we can calculate

$\rho_r = \frac{c}{2B_T} =$ Slant-range resolution

$\rho_v = \frac{\lambda}{2T_{CPI}} =$ Velocity resolution

Velocity resolution depends on the length of the CPI

$B_T =$ Bandwidth of TX signal

$\lambda =$ Nominal wavelength of TX signal

$T_{CPI} =$ Time duration of the CPI

21

21

Processing Extensions – Window Taper Functions

To prevent inadvertent detection of processing sidelobes as targets, i.e. false alarms, we wish to suppress the processing sidelobes by using window taper functions, both in range processing and velocity/Doppler processing.

The penalty is a slight reduction in SNR, hence reduced sensitivity.

Pictured here is the IPR of a -70 dB Taylor window with "no window" and Hamming window as reference.

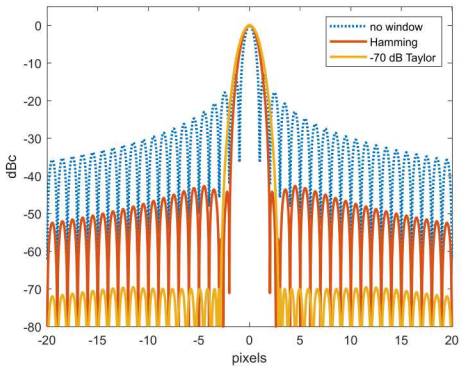

WINDOW SPECTRUM CHARACTERISTICS -70 dB Taylor window (nbar = 11)

half-power bandwidth = 1.5717 (normalized to 1/T)
-3 dB bandwidth = 1.5691 (normalized to 1/T)
-18 dB bandwidth = 3.6449 (normalized to 1/T)
noise bandwidth = 1.6531 (normalized to 1/T)
SNR loss = 2.183 dB
first null = 2.8672 (normalized to 1/T)
PSL = -69.5169 dBc
ISL = -57.4116 dBc from first null outward

22

22

Processing Extensions – Keystone Processing

Recall that an earlier presumption was "Target displacement over a CPI due to its own velocity is less than the range resolution"

If we violate this condition, the simple processing described earlier would smear the IPR in range and velocity, thereby reducing its SNR in any one pixel, and reducing its detectability.

This would get worse for larger target velocities.

This problem is analogous to range-migration in SAR processing. In SAR this is addressed by "Polar Format" processing. The equivalent algorithm for GMTI is "Keystone Processing."

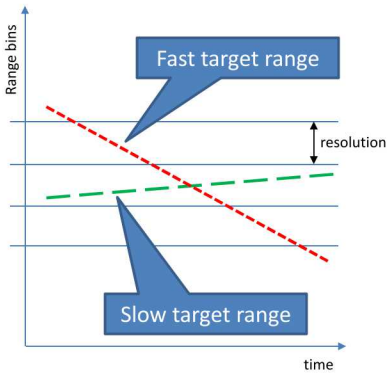

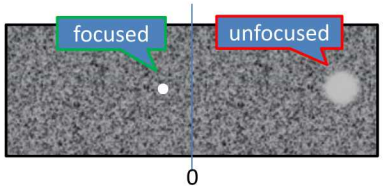

23

23

Processing Extensions – Keystone Processing

The essence of Keystone processing is easiest seen by assuming the employment of a Linear-FM chirp modulation, where

$$\Phi(t) = \frac{\gamma_T}{2} t^2$$

By dechirping and down-converting to baseband, and ignoring some inconsequential phase terms, operating with a constant PRF, and sampling the individual pulse data, the resulting GMTI data can be modelled as

Fasttime index — ADC sample period — Pulse Repetition Interval (PRI)

$$x_V(i,n) \approx A_r \exp j\left(-\frac{2}{c}\gamma_T\left(r_{s,ref} - r_c\right)T_s i - \frac{2}{c}\omega_T\left(1+\frac{\gamma_T}{\omega_T}T_s i\right)v_r T_p n\right)$$

$$= A_r \exp j\left(k_r\left(r_{s,ref} - r_c\right) + k_v v_r\right)$$

where $\begin{cases} k_r = -\frac{2}{c}\gamma_T T_s i \\ k_v = -\frac{2}{c}\omega_T\left(1+\frac{\gamma_T}{\omega_T}T_s i\right)T_p n \end{cases}$

The problem is that we have a cross-coupling of indices here

24

24

Processing Extensions – Keystone Processing

The natural processing of this data is with a 2D-DFT. Efficient processing decouples the 2D-DFT into orthogonal 1D-DFT operations. This implies that we desire the data samples themselves to be on a rectangular grid, i.e. sample locations with decoupled indices in the two dimensions.

The problem:

The cross-coupling of fast-time and slow-time indices causes a smearing in the range-velocity map that gets worse for greater velocities.

This smearing would not happen if the data indices were not cross-coupled.

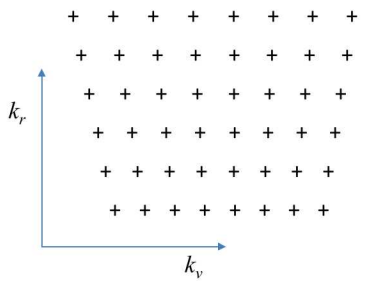

If we plot the k_r and k_v samples onto a grid, their locations appear on a trapezoidal, or "keystone" grid.

Digital Signal Processing, especially when using DFT algorithms, likes data on a rectangular grid.

25

25

Processing Extensions – Keystone Processing

The answer is to interpolate the data onto a rectangular grid.

Mathematically, this creates a new index such that

$$-\frac{2}{c}\omega_T\left(1+\frac{\gamma_T}{\omega_T}T_s i\right)T_p n = -\frac{2}{c}\omega_T T_p n'$$

old index

new index

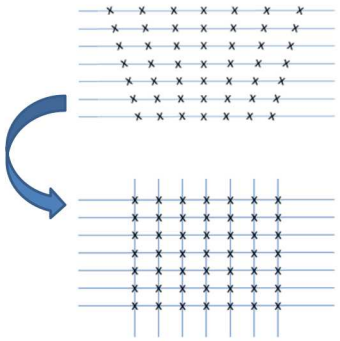

The new data model is

$$x_V(i,n) \approx A_r \exp j\left(-\frac{2}{c}\gamma_T\left(r_{s,ref}-r_c\right)T_s i - \frac{2}{c}\omega_T v_r T_p n'\right)$$

With indices now decoupled, a 2D-DFT which is decoupled into orthogonal 1D-DFT operations will not result in the smearing with increased velocities.

26

26

Processing Extensions – Keystone Processing

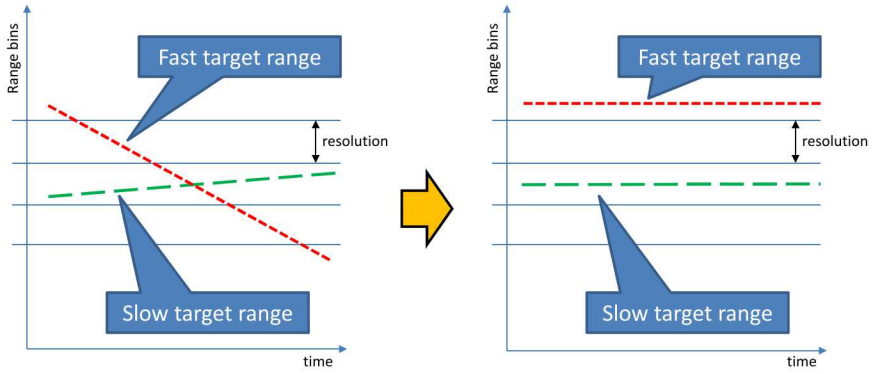

With the keystone to rectangular grid resampling, range has been stabilized for all velocities. This causes targets to focus better in range-velocity images (maps). Different velocities still manifest different phase rates.

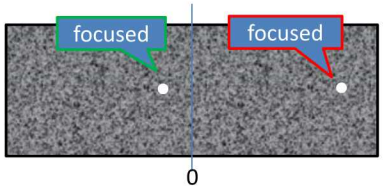

27

27

Static Targets (no target motion)

This is the Synthetic Aperture Radar (SAR) case.

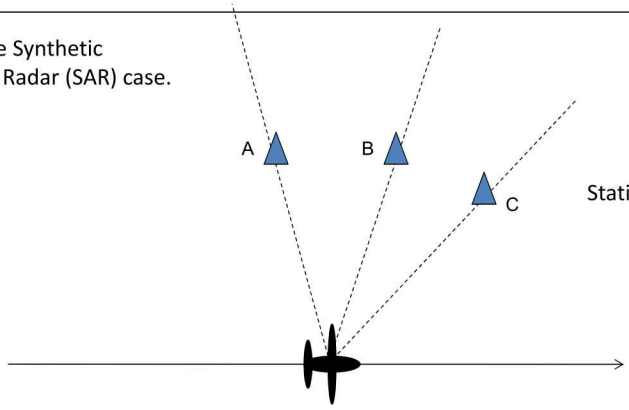

Stationary targets A, B, and C are all being approached by the radar at different rates. They all exhibit different velocities to the radar.

A filter set for different velocities will isolate and separate the different targets.

28

28

SAR Refresh

A SAR image is just the answer to the question "How much echo energy is there at different pairs of 'range' and 'velocity'.

However, the 'image' is usually restricted to range and velocity combinations that are within the antenna beam illumination footprint.

The assumption is static reflectors.

All echoes are presumed to be from static reflectors

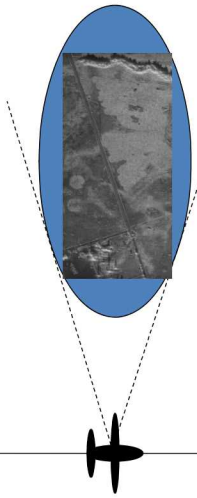

A SAR image is an echo energy map with dimensions of Range and Doppler…

Equivalently, dimensions of Range and Velocity.

Velocity, Doppler, and Direction of Arrival (DOA) are all proportional to each other for static targets.

29

29

If we create a SAR image beyond the antenna footprint, then we are measuring echo energy corresponding to range and velocity for which little or no echo energy should exist (assuming static reflectors).

All we should see is Noise…

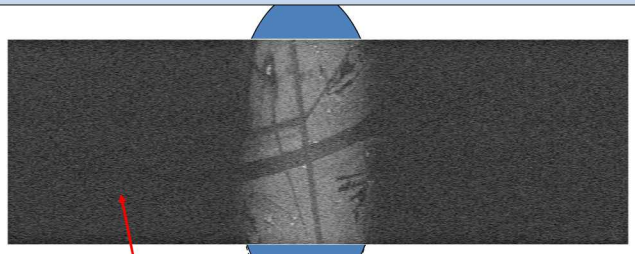

Noise region outside of antenna beam footprint

The image is composed of complex-valued pixels.

The noise is assumed to be complex valued zero-mean Additive Gaussian noise.

30

30

SAR Refresh

The SAR image usually throws away the exo-clutter region before displaying some subset of the endo-clutter region.

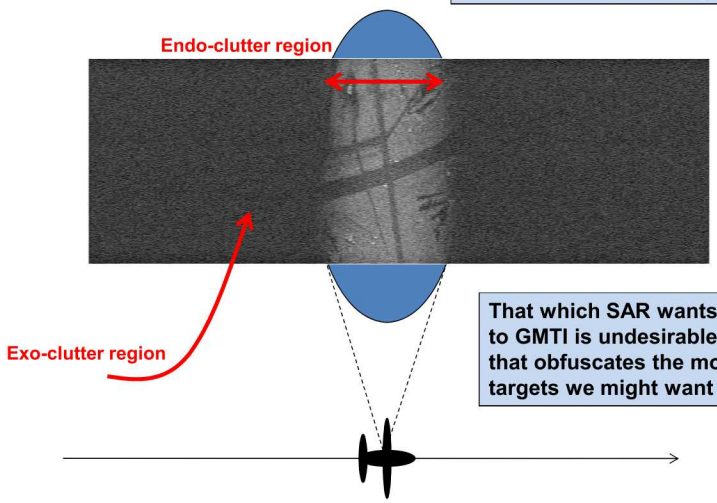

That which SAR wants to keep, to GMTI is undesirable "clutter" that obfuscates the moving targets we might want to detect.

31

31

Moving Reflectors

If a target is moving, it is going to have a relative velocity that is
1. Due to its location, because of radar motion,
   -- AND--
2. Due to its own motion.

The radar is going to map its energy to its range and 'total' velocity.

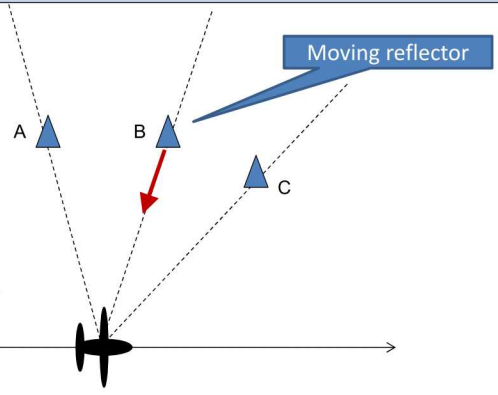

A target's motion decouples its DOA from Doppler and Velocity.

32

32

Moving Reflectors

Note that it is NOT the absolute speed of the vehicle that is important.

Rather, it is the rate at which it is closing with the radar compared to the stationary clutter around it. This will typically be less than the vehicle's ground speed.

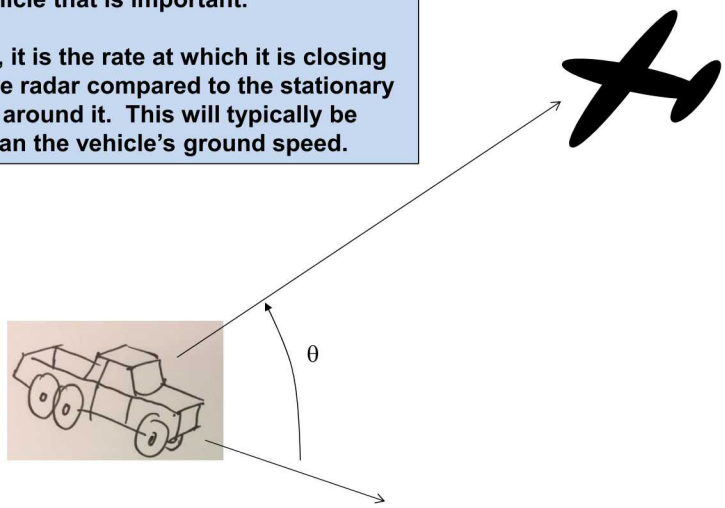

33

33

Moving Reflectors

A Moving target will have its energy mapped to a position in the range-velocity map that corresponds to its TOTAL velocity.

It will be mapped to a velocity that is different than the velocity due just to its location, i.e. with respect to the velocity of the clutter around it. The fact that the target is moving will cause its energy to shift in the clutter 'image'.

A moving target's echo energy will be shifted in a Range-Doppler map with respect to the surrounding clutter.

They will be shifted one way if velocity is towards the radar. They will be shifted the other way if the velocity is away from the radar.

The amount of shift is proportional to the velocity towards or away from the radar.

34

34

GMTI Range-Doppler Map

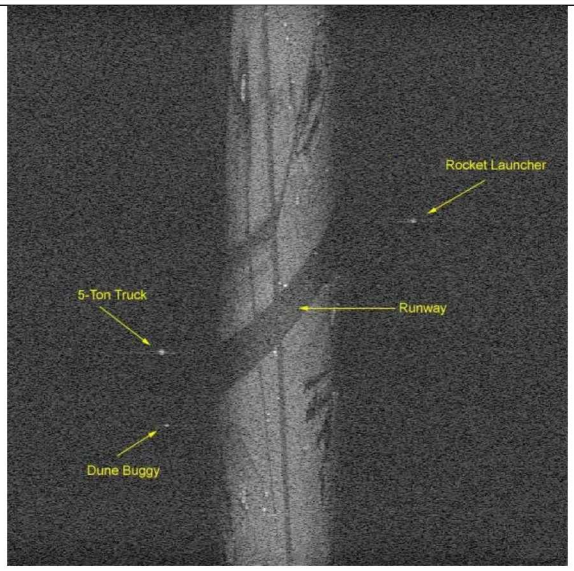

Ground Truth

35

35

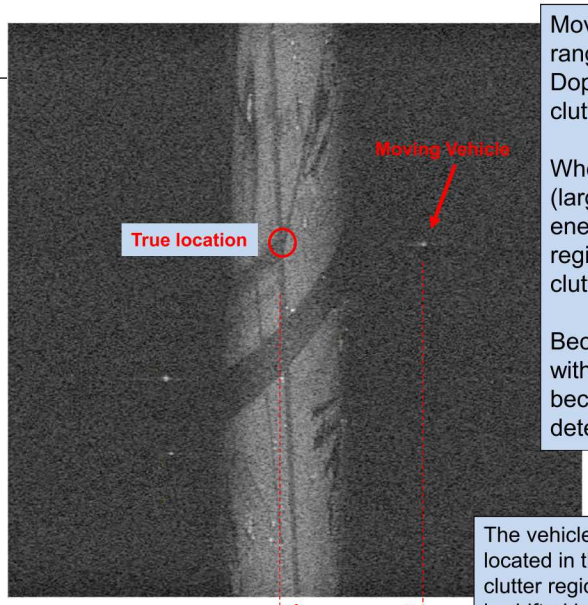

Moving objects with linear range-change are 'shifted' in Doppler with respect to the clutter.

When shifted far enough (large enough velocity), their energy falls outside the region that stationary (static) clutter occupies.

Because they then compete with just noise, these become relatively easy to detect, if bright enough.

The vehicle is actually located in the illuminated clutter region, but its energy is shifted by its own motion.

36

36

GMTI Range-Doppler Map

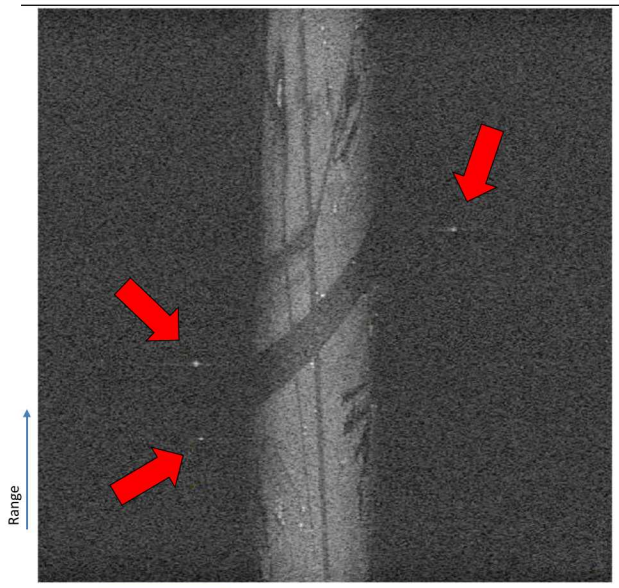

If moving targets are moving fast enough so their energy is shifted out of the antenna beam clutter (into the exo-clutter region), then we can detect them relatively easily.

We definitely want to detect the moving targets, but we don't want to inadvertently declare a detection of some or any stationary clutter.

37

37

GMTI Range-Doppler Map

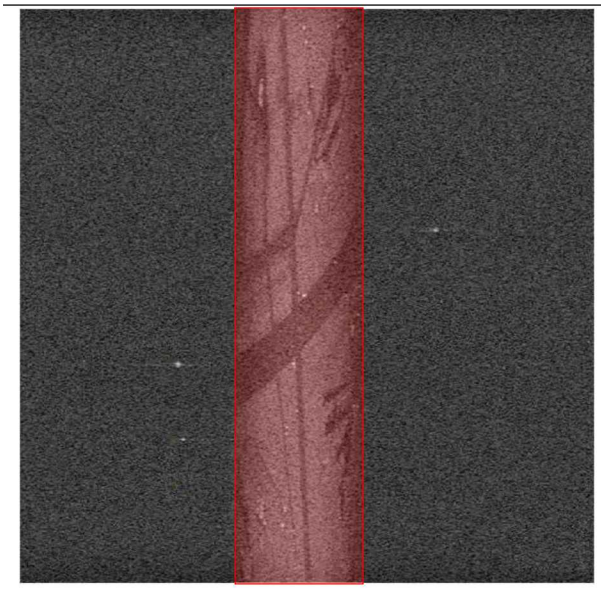

So, the simple GMTI algorithm will generally 'cut out' the clutter region, and not attempt to detect anything inside of this region.

Detections are limited to outside the 'endo-clutter' region.

This, of course, requires knowing where the clutter region is in range and velocity.

38

38

GMTI Products

GMTI normally does not display the range-velocity map as a data product.

Rather, the range-velocity map is an intermediary product on the way to an automatic detection system.

The GMTI product is typically just 'detection reports' with suitable metadata (e.g. RCS estimate, closing velocity, estimated physical location, etc.).

Detections are then simply displayed on a map, sometimes color-coded, or tagged with metadata, often with tracking (time-history) information.

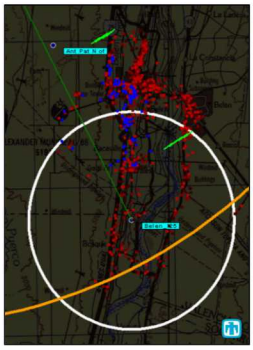

39

39

Detection Theory

At issue is "How do we decide whether a pixel contains a target or not?"

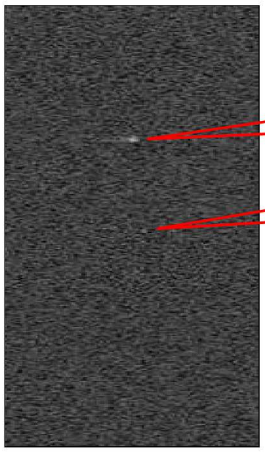

How do we decide that this is a target?

How do we decide that this is 'not' a target?

Recall that the 'image' is complex-valued, and the noise is complex additive Gaussian-distributed, and nearly white (in the sense of perhaps some but little correlation with neighboring pixels).

Ideally, with some caveats

40

40

Detection Theory

The underlying data in the range-velocity image is complex-valued, with I and Q components.

Noise is modelled with a zero-mean 2D Gaussian Probability Density Function (PDF).

The presence of a signal will provide a bias to the noise statistics; the bias having magnitude and phase.

Phase is effectively random, so the only predictable effect of a signal is its magnitude. Consequently, detection is performed on the magnitude of the image.

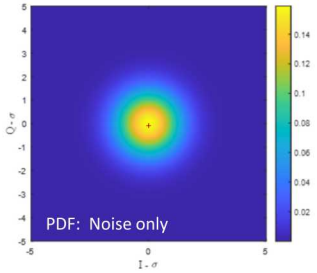

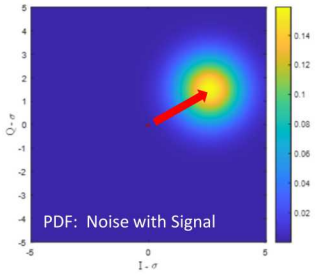

41

41

Detection Theory

The PDF of the magnitude of a complex Gaussian is described by a Rice (or Rician) distribution.

For the noise-only case, this devolves to a Rayleigh distribution.

For the noise-with-signal case, for SNR greater than about 10 dB or so, this can be adequately described by a Gaussian distribution.

(This assumes no post-detection integration)

Our target detection decision is determined by the magnitude of the pixel value; whether the magnitude exceeds some determined threshold.

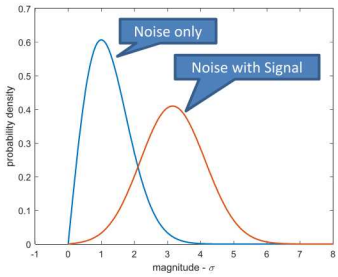

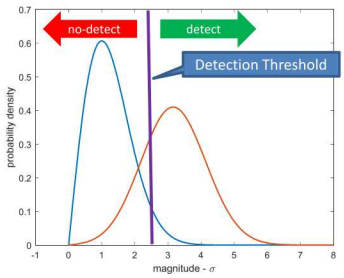

42

42

Detection Theory

Actual probabilities are determined by the area under the PDF curves.

Two important descriptors:

Probability of Detection, P_D

The probability of correctly identifying that a target is present.

Probability of False Alarm, P_{FA}

The probability of incorrectly declaring a target is present when in fact it is not.

Trades:

Increasing P_D will also increase P_{FA}
Decreasing P_{FA} will also decrease P_D

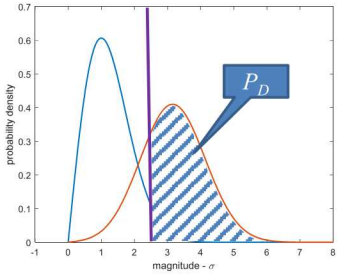

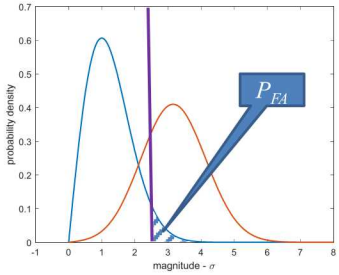

43

43

Detection Theory

The only way to simultaneously increase P_D and/or reduce P_{FA} is to reduce the overlap in the PDFs.

This means increasing the SNR.

The required SNR for specific probabilities (assuming these noise models) is

$$SNR = \left(\sqrt{-\ln\left(P_{FA}\right)} - \frac{Q^{-1}\left(P_D\right)}{\sqrt{2}} \right)^2$$

The inverse-Q-function is defined by

$$Q^{-1}(w) = z \quad \text{where} \quad w = Q(z) = \int_z^{\infty} \frac{1}{\sqrt{2\pi}} e^{-\frac{x^2}{2}} dx$$

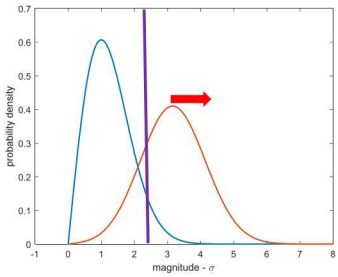

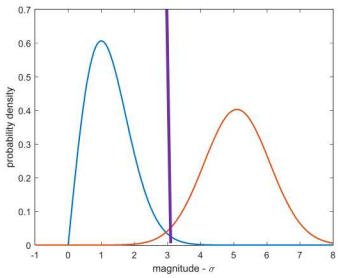

44

44

Detection Theory

Clearly, better SNR allows improving both P_D and P_{FA} at the same time.

Reasonable requirements for machine detection of a single range-velocity map are SNR on the order of 15 to 20 dB.

Reasonable requirements for a human observer, who will also employ contextual information, might be an SNR on the order of 10 to 13 dB.

$$SNR = \left(\sqrt{-\ln(P_{FA})} - \frac{Q^{-1}(P_D)}{\sqrt{2}} \right)^2$$

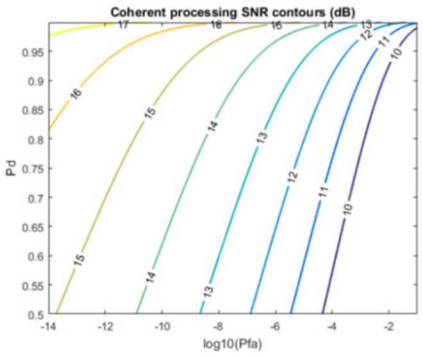

45

45

Detection Theory – False Alarm Rate

Sometimes a more useful measure than P_{FA} is the False-Alarm Rate (FAR).

These are related as

$$FAR = P_{FA} \times (\text{independent tests per second})$$

This can be expanded somewhat to

$$FAR = P_{FA} \times (\text{independent pixels per CPI}) \times (\text{independent CPIs per second})$$

This is really more like the number of resolution cells per CPI

Lower FAR doesn't always mean a better radar, especially since it depends on pixels per CPI and CPIs/sec.

46

46

Detection Theory – CFAR Detector

Usually, the detection threshold is set based on some noise level that allows a tolerable P_{FA}, and hence some tolerable FAR.

If the noise statistics are constant over the entire detection area, then a single common threshold may be employed

$$x_{threshold} = \sigma\sqrt{-\ln\left(P_{FA}\right)}$$

Detection algorithms that use such detection criteria are termed Constant False Alarm Rate (CFAR) detectors.

In addition, especially in good SNR cases, some minimum allowable target Radar Cross Section (RCS) might also be applied.

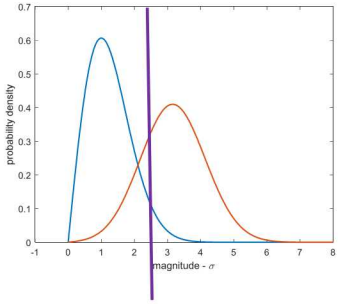

Chosen to yield a constant FAR

47

47

Detection Theory – CFAR Detector

If noise levels are not constant over the entire detection area, then the threshold may be allowed to 'float' based on local noise statistics.

Such detectors are called Cell-Averaged CFAR (CA-CFAR) detectors.

Many configurations exist for selecting regions over which to calculate noise statistics.

It is important to select noise-only regions that don't contain actual target responses. Consequently, "guard" cells are designated to separate the pixel under test from the regions that are presumed to be noise-only.

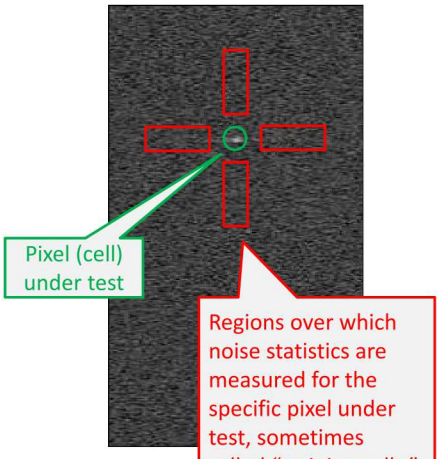

48

48

False Alarms – Other Sources

- **To a radar operator, a false alarm is the apparent detection of 'anything' that he isn't specifically looking for, which for a GMTI radar, is anything that isn't a target of interest to him.**
- **The list of possible sources of false alarms might include any of the following**
  - **System Thermal Noise**
  - **System Phase Noise**
  - **Multiplicative Noise from clutter or targets**
  - **Artifacts from spurs, EMI, etc.**
  - **Strong targets in the antenna sidelobes**
  - **Animals such as flocks of birds, other wildlife, etc.**
  - **Foliage in the wind**
  - **Rotating structures such as turbines, windmills, fans, propellers, etc.**
  - **Other radar antennas**
  - **Vibrating objects such as vent pipes, engine cowlings, etc.**
  - **Rain and other weather effects**
  - **Chaff**
- **In maritime environments, the water itself will move, and move anything in it or on it, including any of the following**
  - **Buoys, Mooring balls**
  - **Floating trash, debris, flotsam, jetsam**
  - **Icebergs, Ice flows**
  - **Breaking waves**
  - **Marine Life**

This is the one on which we focused in the previous analysis

49

49

False Alarms – Clutter Motion

Sometimes stationary clutter isn't all that stationary

up to 0.32 m/s for wooded hills with 40 kt wind,
up to 1.1 m/s for sea echoes,
up to 1.2 m/s for chaff in 25 kt wind, and
up to 4.0 m/s for rain clouds.

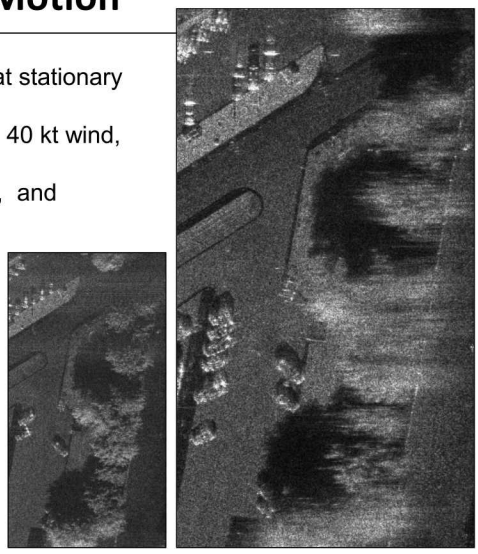

Likely to have more false alarms on windy days

50

50

False Alarms – Spurs, I/Q Purity

What is this?
- Moving Target?
- Bright Stationary target in antenna sidelobe?
- Spurious Response?

Data is never perfect, mainly because hardware is never perfect.

- Antennas have sidelobes, allowing bright stationary reflectors to pose as movers.
- ADCs are not perfectly linear, generating harmonics.
- I and Q data channels are never perfectly balanced.
- Interfering signals leaking/coupling where they shouldn't.

All of these offer the potential to generate false alarms.

False Alarms – Comments

Note that some of these false alarm sources are due simply to uncertainty in the echo energy,

some are due to non-ideal radar performance,

and some are legitimate targets – but simply not the kind of target of interest to the radar operator.

Those due to non-ideal radar performance can be controlled by good design. Good GMTI performance will often require "better" hardware performance than other radar modes, e.g. SAR.

For other False Alarm sources, GMTI systems often employ ad hoc algorithms and heuristics to weed out some of these manifestations.

These are often referred to as False Alarm Mitigation (FAM) techniques.

Detection Decisions

While we have discussed the probability of detection of a target in a single CPI, we recognize that targets exhibit glint and scintillation,

and when multiple CPIs are examined, a decision as to whether a target is present does not require it to be detected in every CPI.

The decision that a target is present then depends on a "cumulative" Probability of Detection.

A popular technique is then the M-of-N detector.

This is a form of post-detection integration

Probability of one detection in N CPIs

$$P_{1of\,N} = 1 - (1 - P_D)^N$$

For example: For a single-CPI P_D of 0.5, detecting at least once in 3 chances yields $P_{1of3} = 87.5\%$

More generally, for an M-of-N detector

$$P_{M\,of\,N} = 1 - \sum_{k=0}^{M-1} \binom{N}{k} P_D{}^k (1 - P_D)^{N-k}$$

$$= \sum_{k=M}^{N} \binom{N}{k} P_D{}^k (1 - P_D)^{N-k}$$

53

53

GMTI Range-Doppler Map – Velocity Measure

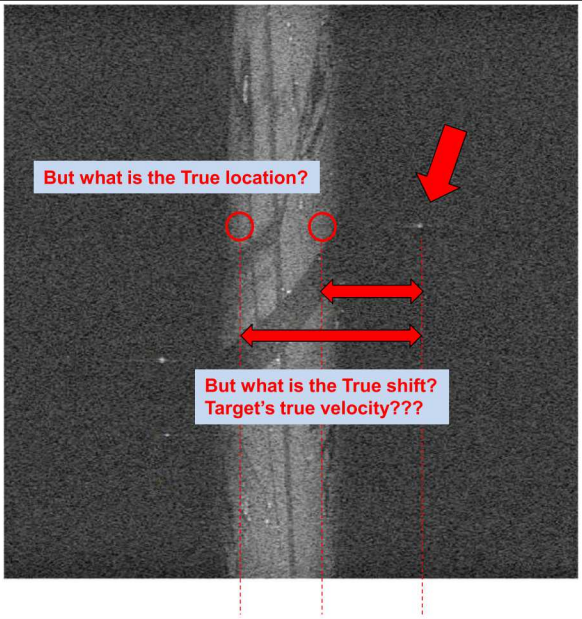

If we don't know the object's true position, we can't really know its true velocity, either.

All we can measure is the total range-rate due to both its position AND its own speed on the ground.

So what do we do?

54

54

GMTI Range-Doppler Map – Velocity Measure

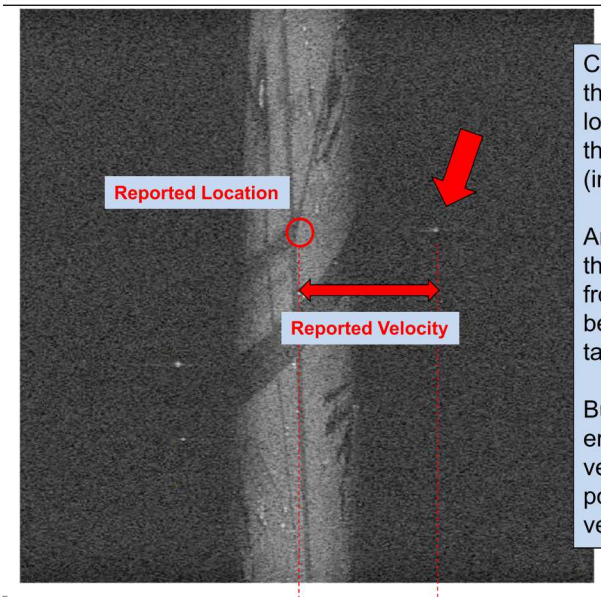

Conventionally, we decide that the 'best guess' object location is in the center of the antenna beam footprint (in azimuth).

And the target velocity is the difference in range-rate from the center of the beam to the detected target's energy.

But this naturally leads to errors in the reported versus actual azimuth position and closing velocity.

55

55

Section Summary

- **There are two principal tasks to basic GMTI operation;**
  - **1) mapping range and velocity into an "image," and**
  - **2) detecting the energy of moving targets.**
- **The image is created by forming a matched filter (or nearly so) against interesting ranges and target velocities.**
- **Target detection is typically implemented via a "Constant False Alarm Rate (CFAR)" detector.**

56

56

Select References

- Catalog of Window Taper Functions for Sidelobe Control
  - Sandia National Laboratories Report SAND2017-4042
- Designing interpolation kernels for SAR data resampling
  - SPIE Proceedings Vol. 8361
- Some comments on GMTI false alarm rate
  - SPIE Proceedings Vol. 8021
- Doppler Characteristics of Sea Clutter,
  - Sandia National Laboratories Report SAND2010-3828
- Earth Curvature and Atmospheric Refraction Effects on Radar Signal Propagation,
  - Sandia National Laboratories Report SAND2012-10690
- Radar Range Measurements in the Atmosphere,
  - Sandia National Laboratories Report SAND2013-1096
- GMTI Processing using Back Projection,
  - Sandia National Laboratories Report SAND2013-5111
- Mitigating I/Q Imbalance in Range-Doppler Images,
  - Sandia National Laboratories Report SAND2014-2252
- Effects of Analog-to-Digital Converter Nonlinearities on Radar Range-Doppler Maps,
  - Sandia National Laboratories Report SAND2014-15909
- Some comments on performance requirements for DMTI radar
  - SPIE Proceedings Vol. 9077

57

57

GMTI Performance Limits

- Radar Equation
- Target statistics – vehicles, dismounts – coherence times
- Swerling numbers
- Blake chart

- MDV
- Blind Velocities
- Aliasing
  - Range
  - Doppler
- Spurious levels

58

58

The Radar Equation

- This is the equation that relates basic radar performance to basic radar parameters
  - i.e. range, resolution, power, etc.
- We will focus on GMTI operation
  - Monostatic
- Used for performance trade studies

59

59

Power Radiation Towards Target

The emitted field expands in a spherical manner, diminishing its power density

$$P_T\left(\frac{1}{L_{TX}}\right)G_A\left(\frac{1}{\sqrt{L_{radome}}}\right)\left(\frac{1}{4\pi R^2}\right)\left(\frac{1}{\sqrt{L_{atmos}}}\right) = \text{TX power density (W/m}^2\text{) at target range}$$

TX Power amplifier output

Loss from TX power amplifier to antenna

Antenna gain

Radome loss

Range to target

Atmospheric loss

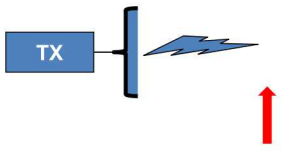

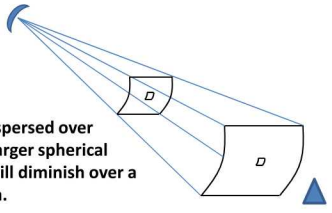

Power dispersed over an ever-larger spherical surface will diminish over a fixed area.

60

60

Interaction With Target

The target captures some of the radiated energy, and then re-radiates it back towards the receiver, i.e. reflection

$$P_T\left[\left(\frac{1}{L_{TX}}\right)G_A\left(\frac{1}{\sqrt{L_{radome}}}\right)\left(\frac{1}{4\pi R^2}\right)\left(\frac{1}{\sqrt{L_{atmos}}}\right)\right]\sigma =$$ Power captured and radiated back towards receiver (W)

Target Radar Cross Section (m^2)

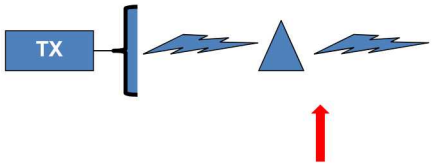

Courtesy of Sandia National Laboratories, Airborne ISR

61

61

Re-radiation Back Towards Receiver

The reflected field expands in a spherical manner, diminishing its power density with range

$$P_T\left[\left(\frac{1}{L_{TX}}\right)G_A\left(\frac{1}{\sqrt{L_{radome}}}\right)\left(\frac{1}{4\pi R^2}\right)\left(\frac{1}{\sqrt{L_{atmos}}}\right)\right]\sigma\left[\left(\frac{1}{\sqrt{L_{atmos}}}\right)\left(\frac{1}{4\pi R^2}\right)\left(\frac{1}{\sqrt{L_{radome}}}\right)\right]$$

= Power density at receiver (W/m^2) with range

We are assuming a single-antenna monostatic radar configuration, i.e. the path from TX to RX is just the reverse of the path from RX to TX.

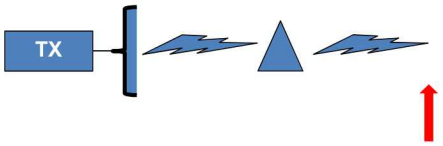

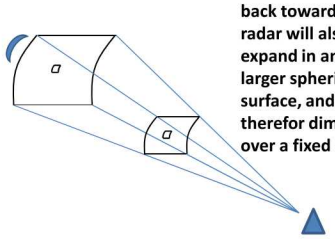

Power re-radiated back towards the radar will also expand in an ever-larger spherical surface, and therefor diminish over a fixed area

62

62

Capture by the Receiving Antenna

The receiving antenna intercepts and collects some of the power in its neighborhood, converting it to power at its terminals.

$$P_T\left[\left(\frac{1}{L_{TX}}\right)G_A\left(\frac{1}{\sqrt{L_{radome}}}\right)\left(\frac{1}{4\pi R^2}\right)\left(\frac{1}{\sqrt{L_{atmos}}}\right)\right]\sigma\left[\left(\frac{1}{\sqrt{L_{atmos}}}\right)\left(\frac{1}{4\pi R^2}\right)\left(\frac{1}{\sqrt{L_{radome}}}\right)\right]A_e$$

= Power captured by RX antenna (W)

Receiver antenna effective area (m^2)

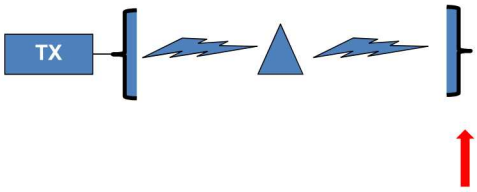

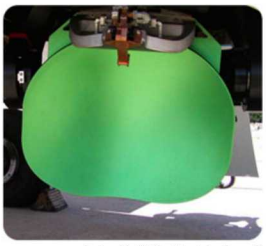

Courtesy of Sandia National Laboratories, Airborne ISR

63

63

Collecting Terms

Collecting some terms and simplifying yields

$$P_r = \frac{P_T G_A A_e \sigma}{(4\pi)^2 R^4}\left(\frac{1}{L_{radar}L_{atmos}}\right) = \text{Signal Power at RX antenna port}$$

where

$L_{radar} = L_{TX}L_{radome} =$ Combined radar system miscellaneous hardware losses

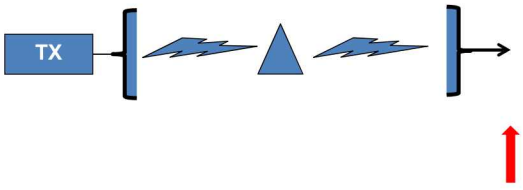

64

64

Competing Noise

The received signal power must compete with noise that is also received and/or generated by the radar… This is added to the signal that is received…

$N_r = kTF_N B_N =$ Noise Power at RX antenna terminals

where

$k = 1.38 \times 10^{-23}$ J/K = Boltzmann's constant

$T = 290$ K = system reference temperature (nominal scene noise temperature)

$F_N =$ System noise factor for receiver (referenced to antenna port)

$B_N =$ Noise bandwidth at antenna port

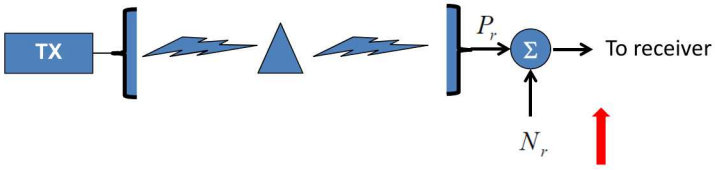

65

65

Noise Sources

- **Thermal emissions from the scene to which the antenna is pointed**
- **Electronic noise in the radar component hardware**
- **Quantization noise due to the ADC**
- **Any additional purposeful noise sources used to perhaps 'dither' the ADC data**

Not included is "multiplicative" noise due to nonlinear nature of radar, integrated sidelobe energy, spurious signals, etc.

66

66

Signal to Noise Ratio (SNR) at RX Antenna Port

An important measure of goodness is the ratio of power (energy) of signal to noise.

$$SNR_{antenna} = \frac{P_r}{N_r} = \frac{P_T G_A A_e \sigma}{(4\pi)^2 R^4 L_{radar} L_{atmos} (kTF_N) B_N}$$

This is a generic form of the Radar Equation that is true for all monostatic radar modes.

67

67

SNR in Range-Velocity Image

The SNR can often be improved by signal processing in a manner to "match" the data to our transmitted signal(s). This involves pulse compression and coherently combining multiple pulses, i.e. GMTI processing.

$$SNR_{image} = SNR_{antenna} G_r G_v = \frac{P_T G_A A_e \sigma G_r G_v}{(4\pi)^2 R^4 L_{radar} L_{atmos} (kTF_N) B_N}$$

where

G_r = SNR gain due to range processing (pulse compression)

G_v = SNR gain due to velocity (Doppler) processing (coherent pulse integration)

The product $G_r G_v$ comprises the signal processing gain

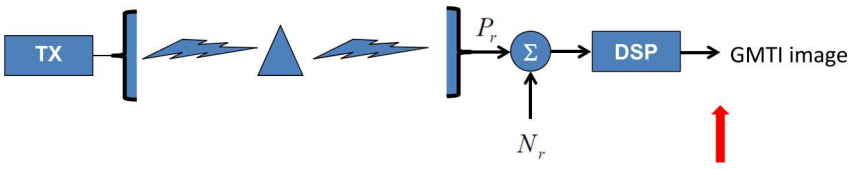

68

68

The Transmitter

The transmitter generally is constrained by 3 main criteria

1. frequency (wavelength) of operation, including bandwidth,
2. peak power output, and
3. maximum duty factor allowed.

We relate

$P_T T_{TX} f_p = P_T d = P_{avg} =$ Average TX power during synthetic aperture

where

$T_{TX} =$ TX pulse width

$f_p =$ Radar Pulse Repetition Frequency (PRF)

$d =$ TX duty factor

69

69

Survey of TX Power Amplifier Tubes

Power Amplifier Tubes

Power Amplifier Tube	Frequency Band of Operation (GHz)	Peak Power (W)	Max Duty Factor	Avg Power (W)
CPI VTU-5010W2	15.2 - 18.2	320	0.35	112
Teledyne MEC 3086	15.5 - 17.9	700	0.35	245
Litton L5869-50	16.25 - 16.75	4000	0.30	1200
Teledyne MTI 3048D	8.7 - 10.5	4000	0.10	400
CPI VTX-5010E	7.5 - 10.5	350	0.35	123
Teledyne MTI3948R	8.7 - 10.5	7000	0.07	490
Litton L5806-50	9.0 - 9.8	9000	0.50	3150[a]
Litton L5901-50	9.6 - 10.2	20000	0.06	1200
Litton L5878-50	5.25 - 5.75	60000	0.035	2100
Teledyne MEC 3082	3.0 - 4.0	10000	0.04	400

Higher peak power usually means lower duty factor
Higher power also usually means narrower bandwidth.

Solid-state power amplifiers are generally lower-power than their tube counterparts, typically under 100 W, and more like 10 W to 20 W range (depending on frequency band). However they do offer a possible efficiency advantage, and technology is advancing to the point where these should be considered for relatively short-range radar applications.

70

70

Antenna Details

For a monostatic radar, TX antenna "gain" and RX antenna "effective area" are related to each other by

$$G_A = \frac{4\pi A_e}{\lambda^2}$$

where

λ = Nominal wavelength of the radar

The "effective area" is related to the physical area of the antenna aperture by an efficiency factor

$$A_e = \eta_{ap} A_A$$

where

A_A = Physical area of antenna aperture

η_{ap} = Aperture efficiency of the antenna (typically on order of 0.5)

Courtesy of Sandia National Laboratories, Airborne ISR

For a dish antenna, the physical aperture is the silhouette area of the dish

71

71

Active Electronic Steered Array (AESA) Antenna

While we have thus far explored traditional corporate fed antennas, many newer systems are using AESA antennas.

While very promising and attractive on a number of fronts, some care needs to nevertheless be exercised when considering AESA antennas for radar application

- AESA have gain and beamwidths that are squint-angle-dependent
- Wideband waveforms require True-Time Delay (TTD) steering, or equivalent. Phase shifters by themselves are inadequate.
- AESA beam-steering does not have the field of regard that a gimballed antenna has.
- AESA antennas still tend to be more expensive than more traditional corporate-fed gimballed antennas.

Nevertheless, since GMTI systems are generally fairly narrow-band, and often require large real-aperture antenna dimensions, AESA antennas are particularly attractive for GMTI systems.

72

72

Signal Bandwidth

The signal bandwidth determines the achievable resolution of the range-compressed signal.

$$B_T = \frac{a_{wr} c}{2\rho_r}$$

where

$c =$ Velocity of propagation

$\rho_r =$ Slant-range resolution

$a_{wr} =$ Range IPR broadening factor due to data tapering (windowing) for sidelobe control

A fundamental rule from Signal Processing is that the Power Spectral Density of a waveform is the Fourier Transform of the Autocorrelation function.

The Autocorrelation function is the output of a matched filter when the input is the signal to which it is matched.

73

73

Processing Gain – Range Compression

The range processing gain is due to noise bandwidth reduction during the course of pulse compression.

$$G_r = \frac{T_{TX} B_N}{L_r}$$

where

$L_r =$ Reduction (loss) in SNR gain due to non-ideal range filtering; a result of using a window taper function for sidelobe control

This gain is based on matched filter performance.

Note that the gain is essentially a time-bandwidth product. However it is the input noise bandwidth that is important, not the signal bandwidth. The typical presumption is that the input noise bandwidth is wider than the signal bandwidth.

74

74

Processing Gain – Pulse Integration

The pulse-integration processing gain is about coherent summation of multiple pulses.

$$G_v = \frac{N}{L_v}$$

where

$N =$ The total number of pulses integrated

$L_v =$ Reduction (loss) in SNR gain due to non-ideal azimuth filtering; a result of using a window taper function for sidelobe control

This gain is based on matched filter performance

75

75

Taylor Window

Window functions are about 'detuning' the filters to get some better sidelobe responses.

The downsides are

1. is slightly worse SNR performance, because after all the net filter isn't precisely matched, and
2. Slightly broadened IPR width, i.e. slightly worse resolution.

One popular window for radar processing is the Taylor window, for which some parameters must also be specified.

Others are also often used.

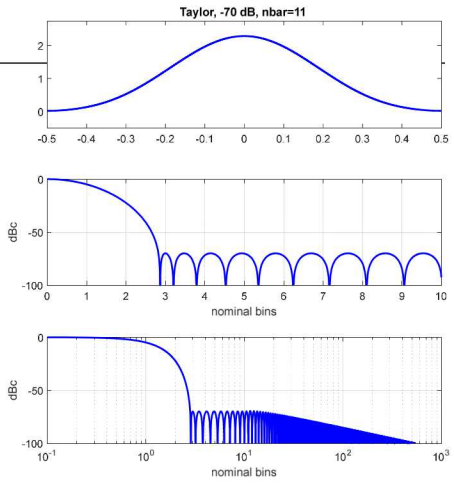

a_{ws}, a_{wr}

L_r, L_v

WINDOW SPECTRUM CHARACTERISTICS

half-power bandwidth = 1.5717 (normalized to 1/T)
-3 dB bandwidth = 1.5691 (normalized to 1/T)
-18 dB bandwidth = 3.6449 (normalized to 1/T)
noise bandwidth = 1.6531 (normalized to 1/T)
SNR loss = 2.183 dB
first null = 2.8672 (normalized to 1/T)
PSL = -69.5169 dBc
ISL = -57.4116 dBc from first null outward

76

76

Radar Cross Section (RCS)

Even for simple targets, a variety of frequency dependencies exist.

RCS frequency dependence

target characteristic	examples	frequency dependence
2 radii of curvature	spheroids	none
1 radius of curvature	cylinders, top hats	f
0 radii of curvature	flat plates, dihedrals, trihedrals	f^2

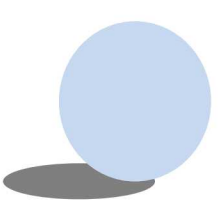

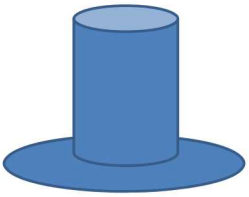

Courtesy of Sandia National Laboratories, Airborne ISR

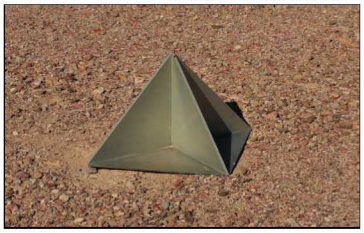

77

77

Radar Cross Section (RCS)

Size matters…

RCS of a sphere as a function of the circumference normalized by the signal wavelength.

In fact, for very small targets, shape doesn't matter.

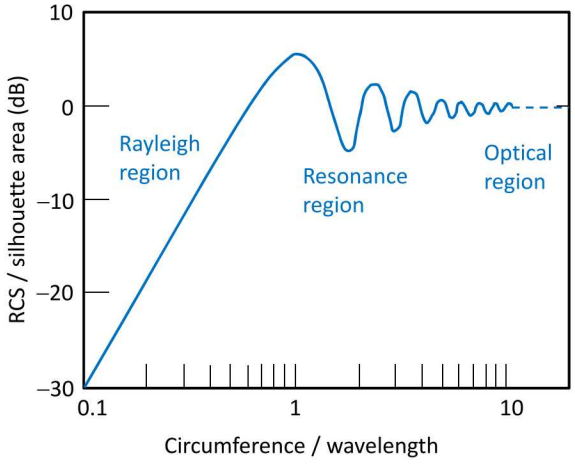

78

78

Swerling Numbers

Complicated targets have complicated RCS behaviors as a function of aspect angle, and are typically described with statistics

- Swerling 1 – many scattering centers without one being dominant, with pulse-to-pulse correlation.
- Swerling 2 – many scattering centers without one being dominant, with no pulse-to-pulse correlation.
- Swerling 3 – many scattering centers but with one being dominant, with pulse-to-pulse correlation.
- Swerling 4 – many scattering centers but with one being dominant, with no pulse-to-pulse correlation.
- The non-fluctuating model is sometimes referred to as Swerling 0, and sometimes as Swerling 5.

$$f_{\text{Swerling\_1}}(\sigma) = \frac{1}{\sigma_{\text{avg}}} e^{-\frac{\sigma}{\sigma_{\text{avg}}}}$$

$$f_{\text{Swerling\_3}}(\sigma) = \frac{4\sigma}{\sigma_{\text{avg}}^2} e^{-\frac{2\sigma}{\sigma_{\text{avg}}}}$$

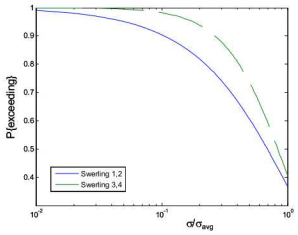

Example:

To reliably detect a 10 percentile average +10 dBsm Swerling 1 target, we need to have adequate SNR to detect 0 dBsm.

79

79

Target Statistics – Vehicles

Anecdotal evidence suggests that vehicles tend to observe a Swerling 1 characteristic, that is, composed of many scattering centers with none being dominant. For some targets, however, such as perhaps a pickup truck with a strong reflection from the interior corner of the bed, a reasonably strong argument can be made for Swerling 3 behavior, that is, composed of a number of scattering centers but with one being dominant.

Raynal, et al., report that for a set of civilian vehicles that included trucks, the median RCS for VV polarization over angle as about +12 dBsm, but varied greatly.

A typical specification for GMTI is to detect a target with average RCS of +10 dBsm, with some high P_D. This would suggest to detecting a minimum RCS of about 0 dBsm with high P_D.

Also important is the coherence time of a vehicle, the time interval for which a target response is reasonably linear phase and reasonably constant amplitude.

At Ku-band, for vehicles, this is typically a fraction of a second.

80

80

Target Statistics – Dismounts

Dismounts tend to exhibit a Swerling 3 target model, with the dominant scattering center being the torso.

The average motion of a dismount torso exhibits the following parameters:

Free Walking Ground Speed = 1.34 ± 0.37 m/s,
Free Walking Ground Speed Range = 0 to 2.1 m/s,
Start and Stop Acceleration = 0.5 m/s^2, and
Free Walking Acceleration = 0.01 to 0.04 m/s^2.

Different than vehicles, the walking dismount is very much not a rigid body.

Raynal, et al., report that for VV polarization at Ku-band, and at 3-m range resolution, 90% of measurements over a number of parameters show an RCS of greater than about −10 dBsm.

A reasonable specification for DMTI is to detect a target with minimum RCS of −10 dBsm, with some high P_D.

A walking human will have a coherence time probably on the order of 100 ms or so

81

81

Miscellaneous Losses

- **Signal Processing Losses**
  - Range & azimuth processing losses due to window functions [typically 2-4 dB or so]
  - Straddling losses (target smeared across several pixels) [often ignored]
- **Radar Losses**
  - Radar plumbing (between TX amplifier and TX antenna) [typically 1-2 dB or so]
  - RX signal path losses often included in system noise factor (figure) [typically 1-2 dB or so]
  - Radome [typically 0.5 dB or so]
- **Atmospheric Losses**
  - Due to the less-than-clear atmosphere
    - Worse losses in adverse weather
    - Very frequency dependent

82

82

Atmospheric Losses

We identify the overall atmospheric loss as

$$L_{atmos} = 10^{\frac{\alpha R}{10}}$$

where

α = two-way atmospheric loss rate in dB per unit distance

Atmospheric loss-rates are very nonlinear with frequency; generally getting worse at higher frequency, with notable peaks at 23 GHz (water absorption line) and about 60 GHz (oxygen absorption lines).

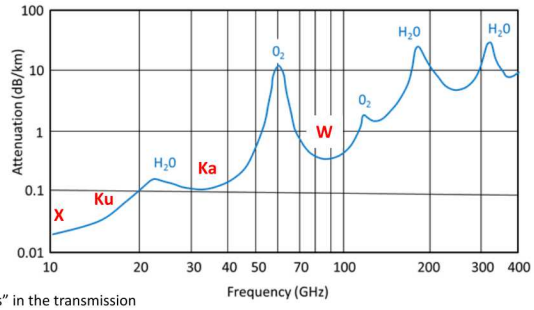

There are some "windows" in the transmission spectrum where we find favored radar bands.

Atmospheric Absorption

Two-way loss rates (dB/km) in 50% RH clear air.

Radar Altitude (kft)	L-band 1.5 GHz	S-band 3.0 GHz	C-band 5.0 GHz	X-band 9.6 GHz	Ku-band 16.7 GHz	Ka-band 35 GHz	W-band 94 GHz
5	0.0119	0.0138	0.0169	0.0235	0.0648	0.1350	0.7101
10	0.0110	0.0126	0.0149	0.0197	0.0498	0.1053	0.5357
15	0.0102	0.0115	0.0133	0.0170	0.0400	0.0857	0.4236
20	0.0095	0.0105	0.0120	0.0149	0.0333	0.0721	0.3476
25	0.0087	0.0096	0.0108	0.0132	0.0282	0.0616	0.2907
30	0.0080	0.0088	0.0099	0.0119	0.0246	0.0541	0.2515
35	0.0074	0.0081	0.0090	0.0108	0.0218	0.0481	0.2214
40	0.0069	0.0075	0.0083	0.0099	0.0196	0.0434	0.1977
45	0.0064	0.0069	0.0076	0.0090	0.0176	0.0392	0.1774
50	0.0059	0.0064	0.0071	0.0083	0.0161	0.0360	0.1617

Atmospheric Absorption

Two-way loss rates (dB/km) in 4 mm/Hr (moderate) rainy weather.

Radar Altitude (kft)	L-band 1.5 GHz	S-band 3.0 GHz	C-band 5.0 GHz	X-band 9.6 GHz	Ku-band 16.7 GHz	Ka-band 35 GHz	W-band 94 GHz
5	0.0135	0.0207	0.0502	0.1315	0.5176	2.1818	8.7812
10	0.0126	0.0193	0.0450	0.1107	0.4062	1.7076	7.7623
15	0.0117	0.0175	0.0391	0.0920	0.3212	1.3311	6.4537
20	0.0106	0.0150	0.0314	0.0714	0.2453	1.0082	4.8836
25	0.0096	0.0132	0.0264	0.0584	0.1979	0.8108	3.9218
30	0.0088	0.0118	0.0228	0.0496	0.1662	0.6788	3.2796
35	0.0081	0.0107	0.0201	0.0431	0.1433	0.5838	2.8178
40	0.0074	0.0098	0.0180	0.0382	0.1259	0.5122	2.4701
45	0.0069	0.0089	0.0163	0.0342	0.1121	0.4558	2.1967
50	0.0064	0.0082	0.0149	0.0310	0.1012	0.4109	1.9793

85

85

Atmospheric Absorption

Two-way loss rates (dB/km) in 16 mm/Hr (heavy) rainy weather.

Radar Altitude (kft)	L-band 1.5 GHz	S-band 3.0 GHz	C-band 5.0 GHz	X-band 9.6 GHz	Ku-band 16.7 GHz	Ka-band 35 GHz	W-band 94 GHz
5	0.0166	0.0373	0.1531	0.4910	1.8857	7.3767	23.0221
10	0.0159	0.0347	0.1282	0.3829	1.4091	5.6330	21.0363
15	0.0146	0.0307	0.1060	0.3020	1.0738	4.3037	17.7448
20	0.0128	0.0249	0.0816	0.2289	0.8097	3.2377	13.3520
25	0.0113	0.0211	0.0665	0.1844	0.6459	2.5944	10.6964
30	0.0102	0.0184	0.0563	0.1546	0.5425	2.1651	8.9251
35	0.0093	0.0163	0.0488	0.1331	0.4658	1.8578	7.6569
40	0.0085	0.0147	0.0431	0.1169	0.4081	1.6269	6.7043
45	0.0078	0.0133	0.0386	0.1042	0.3630	1.4467	5.9604
50	0.0073	0.0122	0.0349	0.0940	0.3270	1.3027	5.3667

86

86

Putting it All Together

There are a number of ways to write the Radar Equation.
Some of these include

$$SNR_{image} = \frac{P_{avg} T_{CPI} \left(\eta_{ap}^2 A_A^2\right) \sigma_{ref} \left(\frac{f}{f_{ref}}\right)^n f^2}{(4\pi) c^2 (kTF_N)(L_{radar} L_r L_a) R^4 10^{\frac{\alpha R}{10}}}$$

or perhaps

$$SNR_{image} = \left(\frac{P_{avg} G_A^2 \lambda^2 T_{CPI} \sigma_{ref}}{(4\pi)^3 (kTF_N) R^4}\right)\left(\frac{1}{L_{radar} 10^{\frac{\alpha R}{10}}}\right)\left[\frac{1}{L_r L_a}\right]\left[\frac{f}{f_{ref}}\right]^n$$

Each has its own utility.

87

87

Comments

- **SNR does not depend on range resolution (for a point target)**
- **PRF can be traded for pulse-width to keep P_{avg} constant**
- **SNR does depend on Doppler resolution. Finer Doppler resolution requires larger T_{CPI}, which improves SNR.**
- **There is no SNR overt dependence on grazing angle, although itself may exhibit some dependence on grazing angle as previously discussed, and atmospheric loss depends on height and range.**
- **Input Noise bandwidth B_N has no direct effect on ultimate image SNR. Signal bandwidth does not explicitly impact SNR directly, but rather through a looser dependence on perhaps L_r.**

88

88

Noise-Equivalent RCS

We define an entity that answers the question
"What equivalent RCS level does the noise look like?"

$$\sigma_N = \frac{\sigma}{SNR_{image}} = \frac{(4\pi)^3 (kTF_N) R^4 L_{radar} L_{atmos} L_r L_a}{P_{avg} G_A^2 \lambda^2 T_{CPI}}$$

In fact, the Noise-Equivalent RCS is the target RCS for which SNR goes to 0 dB.

$$\sigma_N = \sigma\big|_{SNR_{image}=0\,\mathrm{dB}}$$

A typical minimum acceptable noise level for X-band and Ku-band is
– 20 dBsm for vehicles
– 30 dBsm for dismounts

-- lower for lower frequencies.

89

89

Noise-Equivalent RCS Dependencies

We can write the Noise-Equivalent RCS equation as

$$\sigma_N = 64\pi^3 kT \left(\frac{R^4}{T_{CPI}}\right)\left(\frac{F_N L_{radar} L_{atmos}}{P_{avg} G_A^2 \lambda^2}\right)\left(L_r L_a\right)$$

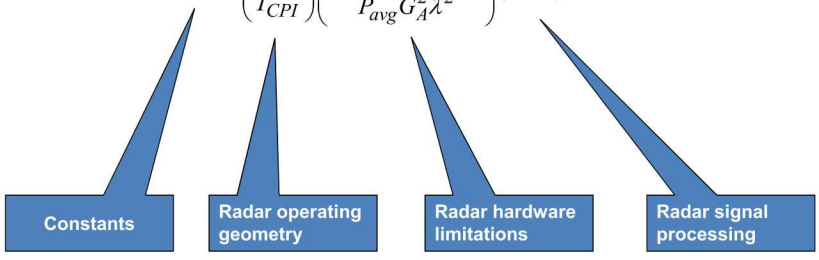

Some of these we can control, and some of them we can't control.

We can probably argue some of these.

90

90

Geometry Limits vs. Noise Levels

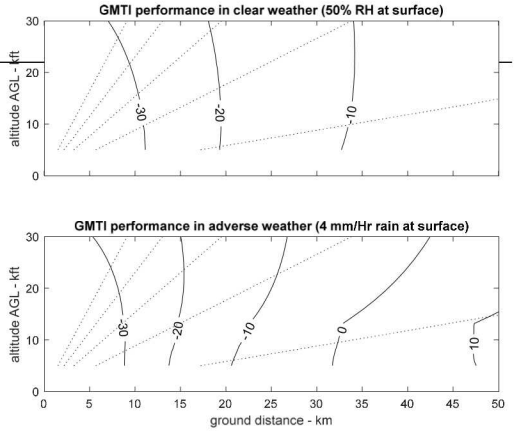

Noise-Equivalent RCS increases with range, and in weather.

Frequency = 16.7 GHz
Power (peak) = 100 W
duty factor = 0.25
Antenna (ap area) = 0.0675 sq m
Antenna (ap aspect) = 3
Antenna (gain) = 31.105 dB

CPI time = 0.1 s
Losses (signal processing) = 3 dB
Losses (radar) = 2 dB
Noise figure = 4.5 dB

(noise RCS in "dBsm")

(default: -20 for vehicles, -30 for dismounts)

91

91

Blake Chart

A tabular form of the Radar Equation is often referred to as a "Blake Chart."

Some sources reserve this term for the Radar Equation rearranged to solve for maximum range.

Others reserve this for a graphical plot.

	units	native format		dB
CONSTANTS				
64*pi^3		1984.401708		32.98
Boltzmann Constant, k	J/K	1.38E-23		-228.60
Reference Temperature, T	K	290		24.62
speed of propagation, c	m/s	3.00E+08		84.77
BASIC PARAMETERS				
frequency	Hz	1.67E+10		
wavelength	m	0.0180		-17.46
TX power - peak	W	100		20.00
duty factor limit	%	25%		-6.02
noise figure	dB	5		5.00
Radar losses	dB	2		2.00
Atmospheric loss	dB	1		1.00
ANTENNA				
Antenna aperture - elevation	m	0.15		
Antenna aperture - azimuth	m	0.450		
Antenna aperture efficiency	%	49.0%		
effective area	m^2	0.033075		
antenna boresight gain		1.29E+03		31.11
RESOLUTION & CPI				
desired resolution - slant range	m	0.30		
Coherent Integration time	s	0.10		-10.00
window function IPR broadening - range		1.57		1.96
window function IPR broadening - Doppler		1.36		1.34
signal bandwidth	Hz	7.84E+08		88.95
Processing Loss - Range	dB	2.18		2.18
Processing Loss - Doppler	dB	1.54		1.54
GEOMETRY CALCULATIONS				
range	m	20000.00		43.01
NOISE CALCULATION				
Noise-equivalent RCS	dBsm			-18.51

92

92

Detectable Velocity

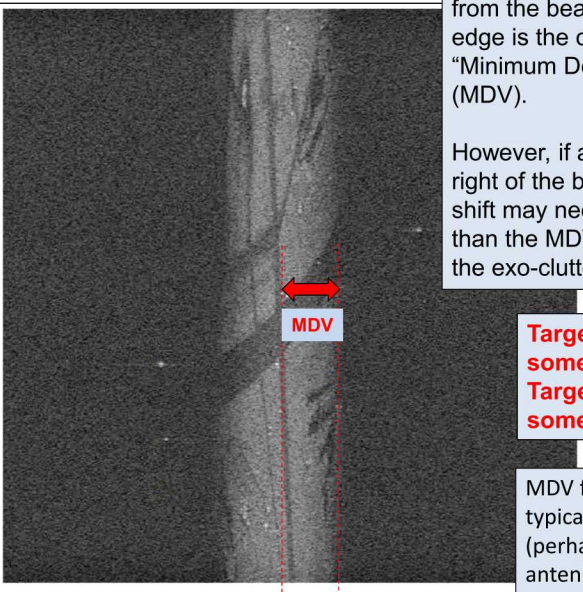

The amount of target velocity that would cause a target's energy to shift from the beam center to the beam edge is the conventionally reported "Minimum Detectable Velocity" (MDV).

However, if a target is located left or right of the beam centerline, then it's shift may need to be more or less than the MDV in order to appear in the exo-clutter region.

Targets > MDV can sometimes be missed, and Targets < MDV can sometimes be detected.

MDV for single-channel GMTI typically corresponds to several (perhaps 3) times the –3 dB antenna beamwidth.

93

93

Detectable Velocity

So… We like narrow clutter regions so that we can have a low MDV.

We can make the clutter region narrower again by using a narrower beamwidth antenna. This means an antenna with larger azimuth dimension; a bigger antenna…

We can also make the clutter region narrower by flying slower. We can mimic this by pointing the antenna closer to the nose of the aircraft.

Ideally, the radar is stationary, i.e. hovering

Courtesy Lockheed Martin

In this manner we can detect some rather slow-moving targets, like people walking (sometimes called "dismounts").

94

94

Detectable Velocity

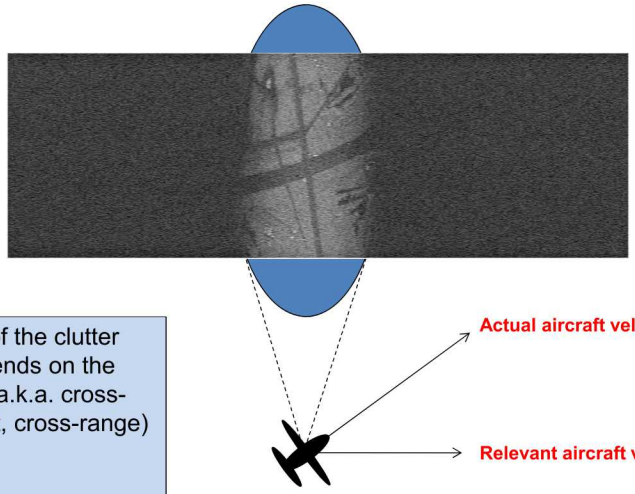

The width of the clutter region depends on the tangential (a.k.a. cross-line-of-sight, cross-range) velocity.

The velocity component in the cross-range direction

MDV is lowest straight-ahead, or straight-behind the aircraft heading.

95

95

Detectable Velocity

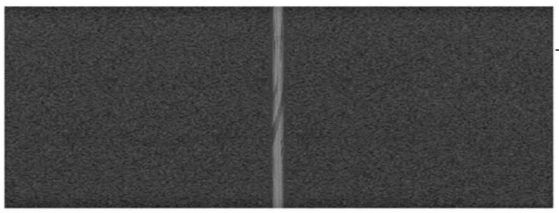

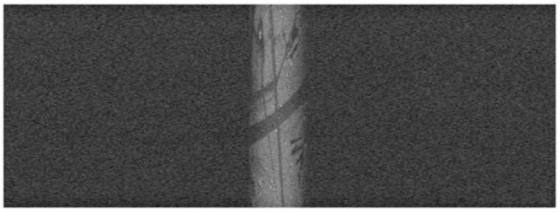

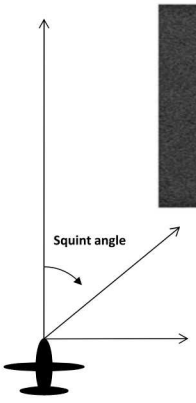

96

96

Detectable Velocity

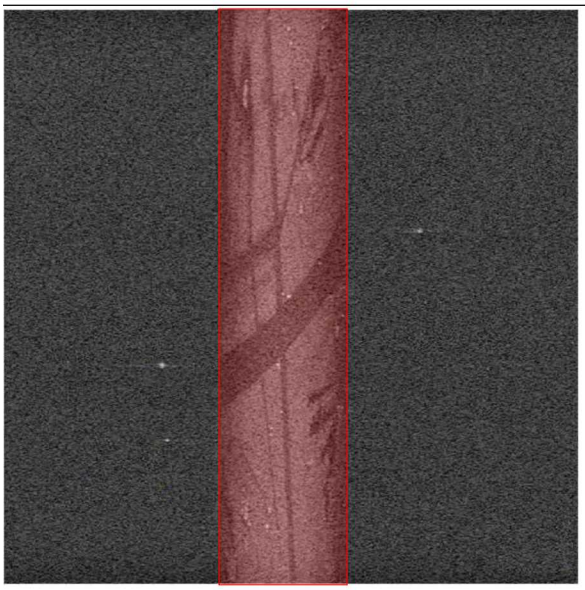

Determining the exclusion region for detections depends on knowing where the clutter region is in range and Doppler.

BUT…

The range and range-rate depends on the radar's viewing geometry… which in turns depends on the scene topography…

97

97

Detectable Velocity

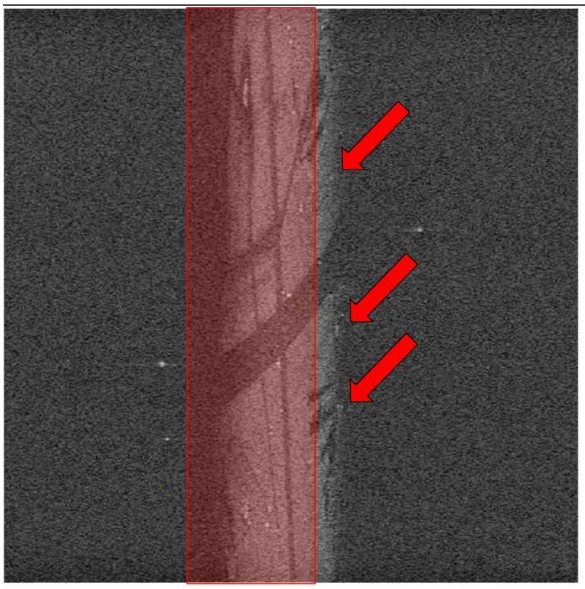

If we get the clutter exclusion region wrong, then we will detect as a moving target some echo energy that is really from a stationary clutter object.

-- increased False Alarms

Or perhaps miss a valid moving target.

-- decreased Probability of Detection

98

Expected clutter region

98

Blind Velocities and Doppler Aliasing

A pulse-Doppler radar is inherently a sampled-data system, with all the characteristics of sampled data. This includes the concepts of replicated spectrum and aliasing, especially when uniform sampling is employed via a constant PRF.

Essentially, as predicted by sampling theory, the spectrums of clutter and targets are replicated at Doppler frequency offsets equal to integer multiples of the radar PRF.

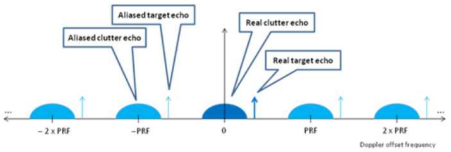

We make two critical observations.

1. Since Doppler corresponds to velocity, any radar echo can be attributed (alias) to multiple possible target velocities as well. There is an inherent velocity ambiguity to the target data.

2. The clutter band represents a region where the radar is 'blind' to moving target echoes. Since the clutter region is replicated and aliased to higher velocities in addition to its true spectral location, there exist 'blind' velocity bands well above the MDV limits previously identified.

99

99

Blind Velocities and Doppler Aliasing

To make blind velocities visible again, we need to change the PRF so as to move the replicated clutter band out of the way.

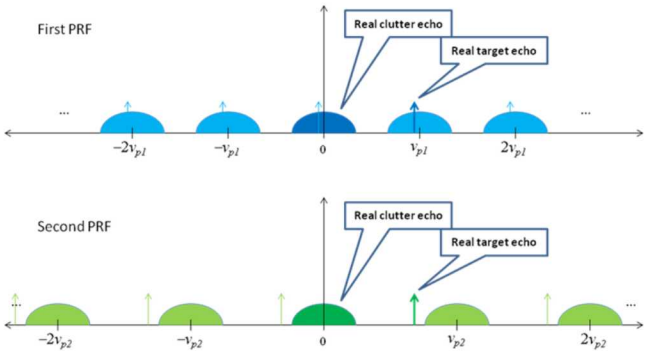

We note that changing radar PRF also allows some degree of mitigation of Doppler ambiguity (aliasing). This is because aliased Doppler returns will scale in Doppler with the changing radar PRF. The true Doppler will not. One technique for resolving the ambiguity is the well-known Chinese Remainder Theorem.

100

100

Range Aliasing

For GMTI we typically desire to have a fairly large exo-clutter region, implying higher PRFs.

This exacerbates range-ambiguities; problems associating an echo with the appropriate transmitted pulse.

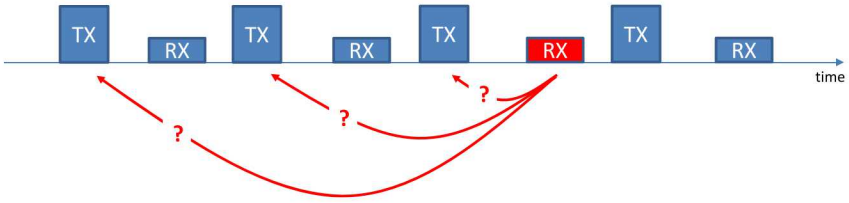

Mitigation schemes might include varying PRF, or phase-coding pulses.

101

101

Topography Effects

Suppose we have an array of stationary corner reflectors on the ground.

What would this clutter look like in a range-Doppler map?

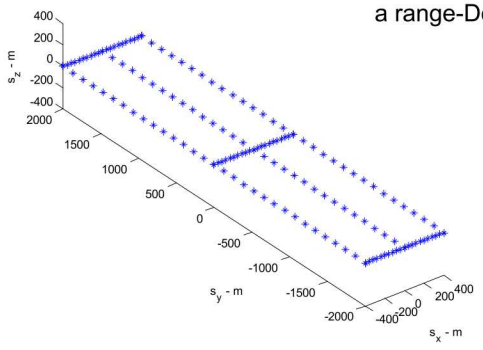

102

102

Topography Effects

If the scene has non-level topography, then the range-Doppler map will reflect this with corresponding range-rate displacements.

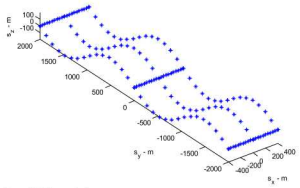

A scene that is tilted in cross-range will exhibit a broadening or narrowing of the clutter band.

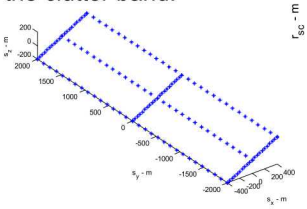

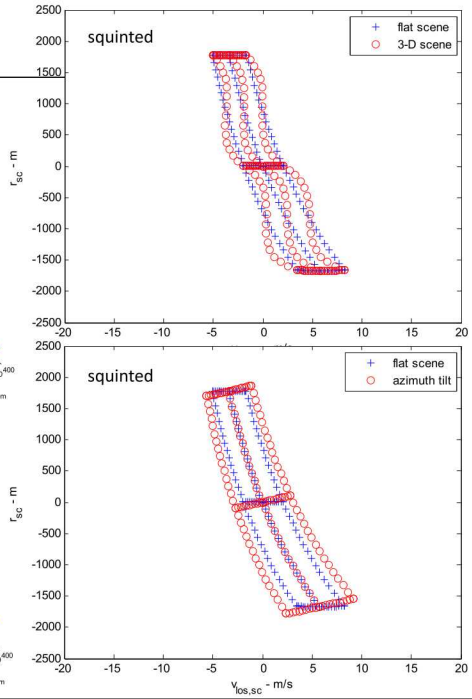

103

103

Topography Effects

Bottom Line:

To minimize False Alarms, and maximize detections, the radar needs to account for topography when deciding where the clutter band is.

The radar needs access to DTED data – especially in mountains.

It's all about accounting for "layover"

DTED = Digital Terrain Elevation Data

104

104

Section Summary

- A common measure for image 'goodness' with respect to SNR is the Noise-Equivalent RCS
  - The target RCS that yields SNR of 0 dB
- The 'range' limit for GMTI depends on the target we wish to detect, and what SNR we need for detection
  - Vehicles: desire Noise-Equivalent RCS of perhaps -20 dBsm
  - Dismounts: desire Noise-Equivalent RCS of perhaps -30 dBsm
- Target Detectability will depend heavily on clutter characteristics
  - and all the things that affect clutter characteristics

105

105

Select References

- Performance Limits for Synthetic Aperture Radar – second edition
  - Sandia National Laboratories Report SAND2006-0821
- Performance Limits for Maritime Inverse Synthetic Aperture Radar (ISAR)
  - Sandia National Laboratories Report SAND2013-9915
- Noise and Noise Figure for Radar Receivers
  - Sandia National Laboratories Report SAND2016-9649
- Radar Receiver Oscillator Phase Noise
  - Sandia National Laboratories Report SAND2018-3614
- Radiometric calibration of range-Doppler radar data
  - Proc. of SPIE, Vol. 11003
- SAR Ambiguous Range Suppression
  - Sandia National Laboratories Report SAND2006-5332
- Radar Doppler Processing with Nonuniform Sampling
  - Sandia National Laboratories Report SAND2017-7851
- Noise and Noise Figure for Radar Receivers,
  - Sandia National Laboratories Report SAND2016-9649
- Radar cross section statistics of dismounts at Ku-band
  - SPIE Proceedings Vol. 8021
- Radar cross section statistics of ground vehicles at Ku-band
  - SPIE 2011 Proceedings Vol. 8021
- Radar cross section statistics of cultural clutter at Ku-band
  - SPIE 2012 Proceedings Vol. 8361
- Discriminating spurious signals in radar data using multiple channels
  - SPIE 2017 Proceedings Vol. 10188

106

106

GMTI Clutter Mitigation

- **Clutter characteristics**
- **Algorithms – DPCA, ATI, STAP**
- **DOA, multi-aperture/beam**
- **Guard Channels**

107

107

CLutter

The bane of GMTI systems is clutter.

Clutter may cause false alarms, and obscure legitimate targets.

Clutter may be categorized into two principal types.

1. Distributed clutter

   e.g. fields, vegetation, etc.

2. Discrete clutter (a.k.a. clutter discretes)

   bright specular reflectors

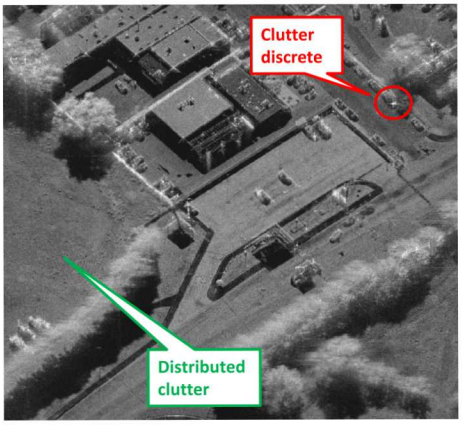

Although often assumed otherwise for convenience, clutter is generally not homogeneous.

108

108

Clutter – Distributed

Distributed clutter is described by a normalized RCS per unit area.

The actual RCS of a pixel of clutter in a range-velocity map depends on the spatial resolution of the clutter cell centered on the pixel.

$$\sigma = \sigma_0 \rho_a \left(\frac{\rho_r}{\cos\psi_g} \right)$$

Range resolution

Grazing angle

Clutter reflectivity

Azimuth spatial resolution

The azimuth spatial resolution is given by $\rho_a = \min\left\{ (R\theta_{az}), \left(\frac{a_{wv}\lambda R}{2 v_x T_{CPI}} \right) \right\}$

Azimuth antenna beamwidth

Cross-range velocity

Distributed clutter is usually modelled as a Gaussian-distributed random process. The characteristic reflectivity is the variance of the associated random variable.

109

109

Clutter – Typical Reflectivity Values

Reflectivity σ_0 values typically depend on frequency, grazing angle, polarization, etc.

Typical values at Ku-band (16.7 GHz) might be

–5 to –10 dBsm/m^2 for urban areas or rocky areas

–10 to –15 dBsm/m^2 for cropland or forest areas

–15 to –20 dBsm/m^2 for grasslands

–20 to –30 dBsm/m^2 for desert areas or road surfaces

110

110

Clutter – Geometry Effects

Typically, the radar is specified to operate at a particular height above the ground. Consequently, grazing angle depends on this height, and the slant-range of operation. For a flat earth this is calculated as

$$\sin\psi_g = \frac{h}{R} \qquad \cos\psi_g = \sqrt{1-\left(\frac{h}{R}\right)^2}$$

where

h = height of the radar above the target

Note that σ_0 also generally has a dependency on grazing angle ψ_g. This is sometimes embodied in a "constant-gamma" model for clutter. In this case the reflectivity is modelled as

$$\sigma_0 = \gamma \sin\psi_g$$

where

γ = Clutter "gamma"

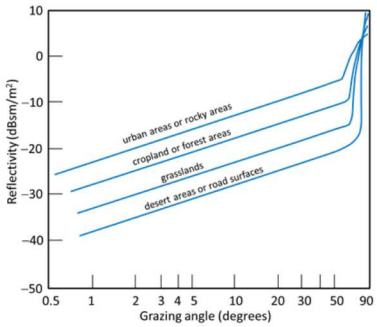

Typical effects of grazing angle on clutter reflectivity

111

111

Clutter – Discretes

Stralka and Fedarke, in Skolnik's Radar Handbook, offer a model for the density of clutter discretes at "higher radar frequencies" given in the following table.

RCS	Density (per sq. mile)
10^6 m² (60 dBsm)	0.01
10^5 m² (50 dBsm)	0.1
10^4 m² (40 dBsm)	1

Raynal, et al., note that a scene containing typically some cultural features will contain clutter discretes that exceed +45 dBsm approximately once per square mile.

Clutter discretes are often bright enough to bleed through antenna sidelobes, thereby manifesting in the exo-clutter region, masquerading as moving targets.

112

112

Clutter and Moving Targets

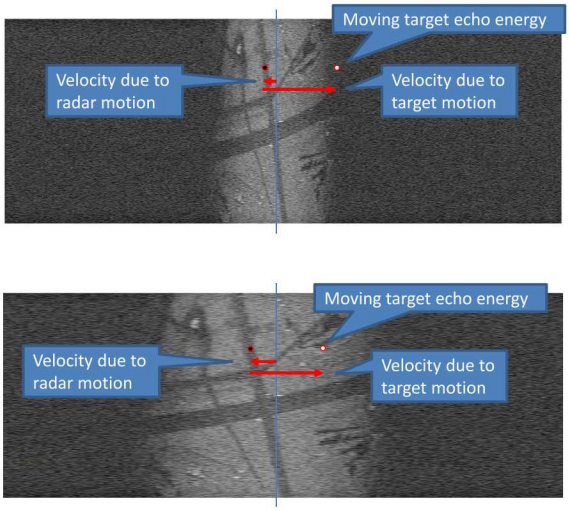

So… The faster the radar flies, the greater is the velocity (Doppler) spread due to position…

This means that the stationary clutter band gets wider in the range-Doppler map

But moving objects do not shift proportionately, and ultimately become enmeshed in the clutter.

Doubling the radar's velocity will double the clutter width, but not double the shift of a moving object. It may even draw the target into the clutter.

113

113

Endo-Clutter Moving Targets

Is this bright spot a stationary object, or is it a moving object that has been shifted only a little bit, just not enough to push its energy into the exo-clutter region?

This suggests that to be clearly identified as a moving object, its energy must be shifted into the exo-clutter region.

This is why we don't like clutter for GMTI.

It must have a minimum velocity in order to be detected – a Minimum Detectable Velocity (MDV)…

114

114

Slow Moving Train In Albuquerque, NM

1 Meter Resolution – September 13, 1996

Range = 5 km, Depression Angle = 9.7°

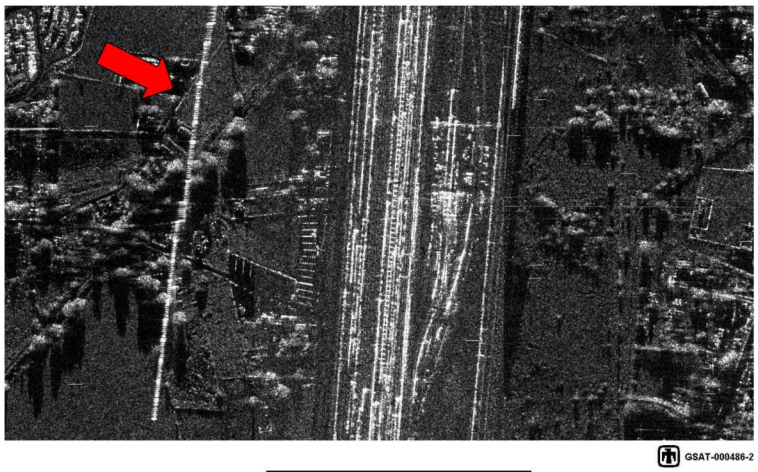

Note the displaced energy due to train motion.

115

115

Endo-Clutter Moving Targets

Reducing MDV

Sometimes we want to detect some very slow-moving targets, like people (or "dismounts") walking.

These have small RCS, 0 dBsm to -10 dBsm,

and move with low velocities, less than 1 m/s.

Dismount Moving Target Indicator (DMTI) radar.

DMTI is just GMTI for people targets…

With a single-beam antenna, we would need some combination of

1. Large antenna
2. Slow radar velocity
3. Limited to forward or aft squint angles

Sometimes we need "more"

116

116

Endo-Clutter Moving Targets

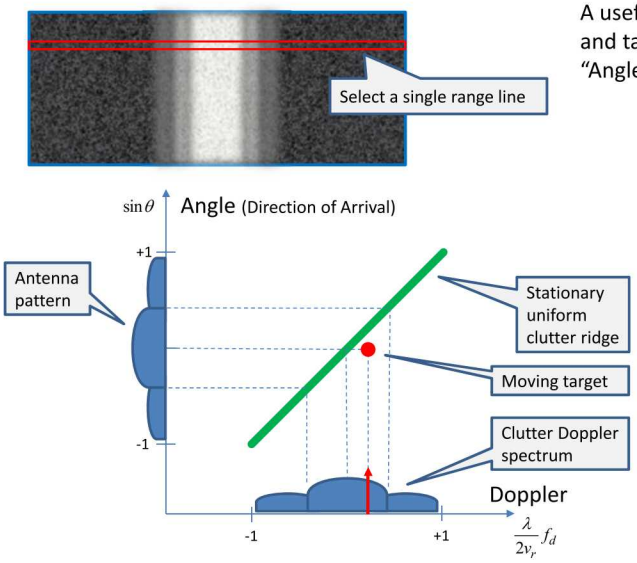

A useful representation of clutter and target characteristics is the "Angle-Doppler Spectrum."

This suggests that moving targets and stationary clutter should be separable, given adequate information to do so.

117

117

Reducing MDV

An alternative is to use a more exotic GMTI scheme.

We essentially need to separate or discriminate the energy of the stationary clutter from the energy of the slow-moving vehicle or dismount.

This requires another degree of freedom, that is, another source of information. This is accomplished with a multi-phase-center (or multi-beam) antenna and a multi-channel radar system. This is a more complex hardware and software solution.

A new dimension to the data

118

118

Clutter Cancellation/Suppression

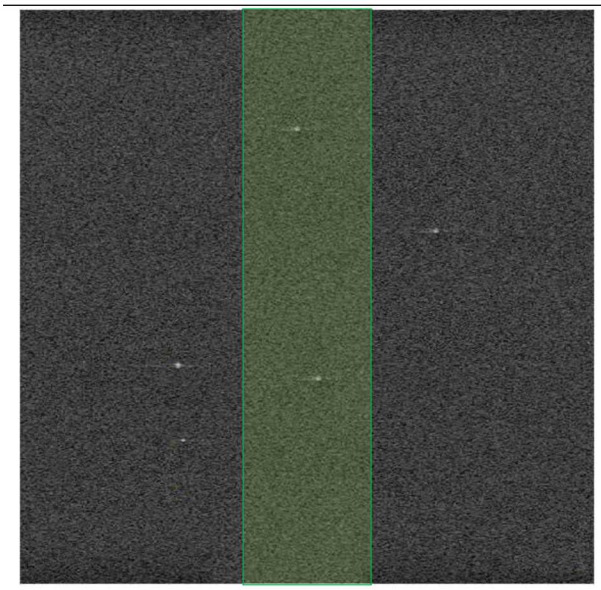

Clutter band region

If clutter is sufficiently cancelled or suppressed (filtered), the moving targets become 'visible' again.

These techniques are generically called "Endo-clutter" GMTI techniques.

Such systems are typical for fast-moving platforms, such as J-STARS, GlobalHawk, and orbital GMTI concepts.

These systems are harder to design, build, calibrate, etc.

119

119

Range-Doppler map

Clutter-cancelled map

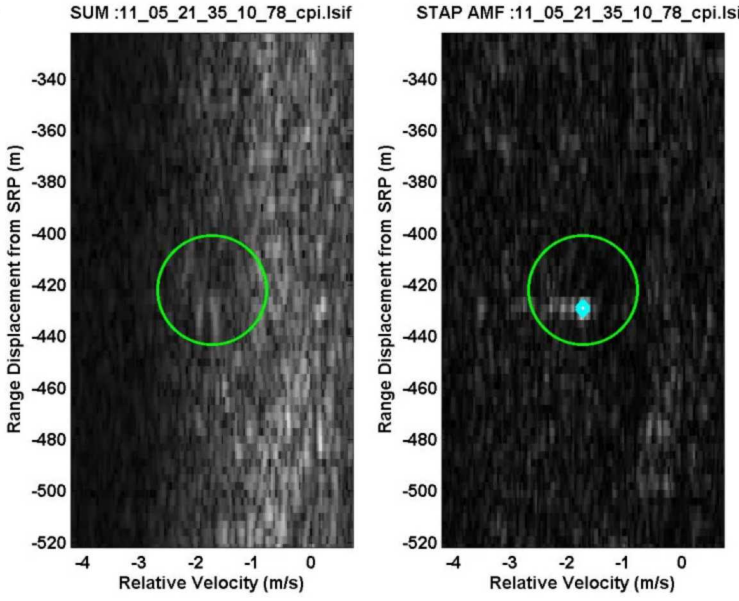

120

120

Clutter Cancellation/Suppression

For example, we can take two separate SAR images of the same scene, but at slightly different times, but equal in all other respects.

Whatever is different between the two images must be due to something that has moved, even if by only a fraction of a wavelength. [change detection]

The basic idea for detecting moving targets in the endo-clutter region is to:

Make two (or more) range-Doppler maps
From essentially the same place in space (along same flight path)
But at slightly different times (i.e. front-half and back-half of antenna)

Complex pixels that 'match' are identified as '**clutter**'. By mapping the "mis-match" in the range-Doppler map, we have essentially cancelled, or suppressed, stationary (static) clutter.

Pixels that 'don't match' in the range-Doppler map are identified as '**moving objects**'.

Having the second range-Doppler map yields an extra degree of freedom - an extra amount of information to allow separating stationary clutter from moving targets.

121

121

Clutter Cancellation/Suppression

All practical GMTI processing algorithms have in common the notion that we have 'multiple' simultaneous perspectives (antennas) along with multiple time history of pulses for each of them.

In this manner, we can somewhat decouple 'space' from 'time.'

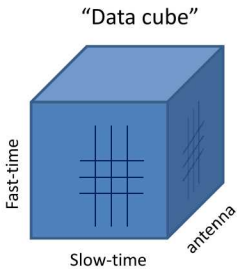

This, of course, means we need to process across both dimensions of 'space' and 'time.'

Space-Time Processing

Gives us an angle measure

Gives us a Doppler measure

122

122

Clutter Cancellation/Suppression

There are a variety of processing algorithms for multiple antenna phase centers, or multiple antenna beams.

These go by various names, like

1. **Displaced Phase Center Antenna (DPCA)**
2. **Along Track Interferometry (ATI)**
3. **Space-Time Adaptive Processing (STAP)**

All are related and essentially try to do the same thing; look for reflectors that do not behave as static clutter.

123

123

Processing – DPCA (Displaced Phase Center Antenna)

Consider two antenna phase-centers flying the same flight path, but with phase centers displaced in along-track position.

Phase centers reach the same position at different times.

Range-compressed signal

$$x_V\left(\hat{r}_{s,ref},n,m\right)=\left\{\begin{array}{l} A_r W_r\left(\dfrac{r_{s,ref}-\hat{r}_{s,ref}}{\rho_r}\right) \\ \times\exp j\left(-\dfrac{2\omega_T}{c}\left[v_s T_p n-\left(v_a T_p n+\dfrac{b}{2}m\right)\sin\theta\right]\right)\end{array}\right\}$$

baseline

Phase-center index

$m\in\{0,1\}$

PRI

DOA relative to broadside

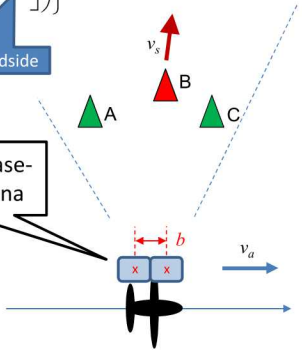

Displaced phase-center antenna

DPCA depends on phase-centers being aligned in "space" rather than time.

124

124

Processing – DPCA

Consequently we define a new index to spatially align the data

$$n' = n + \frac{b\,m}{2v_a T_p}$$

Interpolation operation, but made easier for integer offsets

This allows us to make model variations due to index m depend on only target velocity.

The new data model becomes

$$x_V\left(\hat{r}_{s,ref}, n', m\right) = A_r W_r\left(\frac{r_{s,ref} - \hat{r}_{s,ref}}{\rho_r}\right)\exp j\left(-\frac{2\omega_T}{c}\left[v_s - v_a \sin\theta\right]T_p n'\right)\exp j\left(\frac{2\omega_T}{c}\left[\frac{v_s b}{2v_a}\right]m\right)$$

Now we look at the difference between the signals from the two phase centers

Note that amplitude now depends on target velocity

$$\begin{pmatrix} x_V\left(\hat{r}_{s,ref}, n', 1\right) \\ -x_V\left(\hat{r}_{s,ref}, n', 0\right) \end{pmatrix} = \left\{\begin{array}{l} 2jA_r W_r\left(\frac{r_{s,ref} - \hat{r}_{s,ref}}{\rho_r}\right)\sin\left(\frac{\omega_T}{c}\left[\frac{v_s b}{2v_a}\right]\right) \\ \times\exp j\left(-\frac{2\omega_T}{c}\left[v_s - v_a\sin\theta\right]T_p n'\right)\exp j\left(\frac{\omega_T}{c}\left[\frac{v_s b}{2v_a}\right]\right) \end{array}\right\}$$

Single-delay canceller. (More elaborate schemes exist)

125

125

Processing – DPCA

The term $\sin\left(\frac{\omega_T}{c}\left[\frac{v_s b}{2v_a}\right]\right)$ acts as a target-velocity filter

Assume that the baseline is half the antenna dimension

Clutter, for which this term is zero, is effectively nulled. However, almost all target velocities are attenuated somewhat. Slower velocities more so.

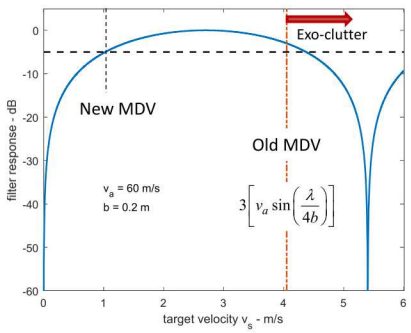

Target detectability becomes more dependent on SNR.

Somewhat conventionally, a rule of thumb becomes the new MDV is at the target velocity that manifests a 5 dB reduction in SNR.

However, targets with sufficient SNR after attenuation are detectable at slower velocities than this.

126

126

Processing – DPCA

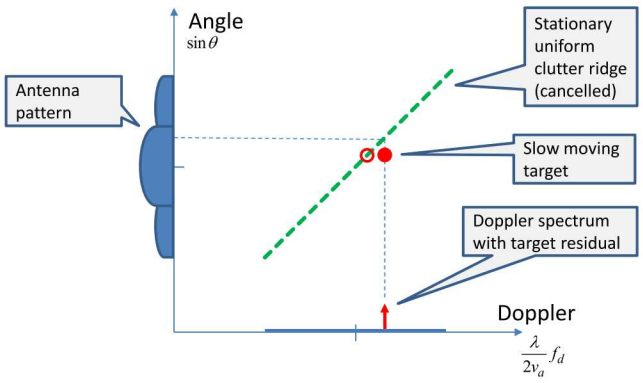

127

127

Processing – DPCA relationship to CCD

Differencing is a similarity measure, very related to measuring coherence.

Instead of flying two antennae on one pass, we could fly one antenna on two passes. Doing so, and measuring coherence between the images is simply SAR Coherent Change Detection (CCD).

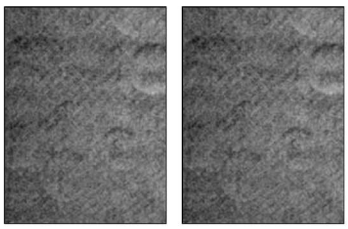

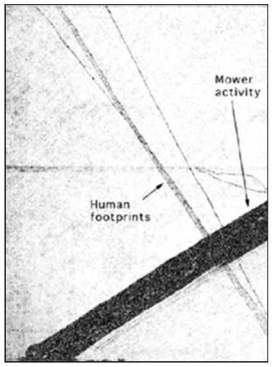

For images, we calculate the coherence of pixel (m,n) using a local neighborhood of K points around the pixel

$$\mu(m,n) = \frac{\left|\sum_{k\in K} x_k^* y_k\right|}{\sqrt{\sum_{k\in K} x_k^* x_k \sum_{k\in K} y_k^* y_k}}$$

This is an estimate of the total coherence of pixel (m,n)

128

128

Processing – ATI (Along-Track Interferometry)

Consider two antenna phase-centers flying the same flight path, but with phase centers displaced in along-track position.

Phase centers form an interferometer.

Range-velocity "image"

$$x_V\left(\hat{r}_{s,ref},\hat{v}_r,m\right) \approx A_r W_r\left(\frac{r_{s,ref}-\hat{r}_{s,ref}}{\rho_r}\right) W_v\left(\frac{\left(v_s - v_a\sin\theta\right)-\hat{v}_r}{\rho_v}\right)\exp j\left(\frac{2\omega_T}{c}\left[\frac{b\,m}{2}\sin\theta\right]\right)$$

Phase-center index

$$m \in \{0,1\}$$

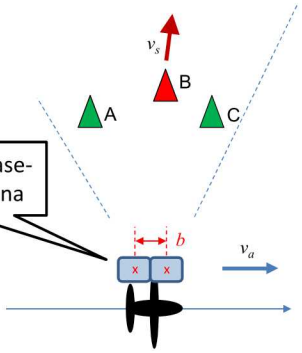

ATI depends on phase-centers being aligned in time rather than space (different than DPCA).

129

129

Processing – ATI

Now we look at the Interferometric phase difference between the signals from the two phase centers

Note that the DOA does not depend on any velocities

$$\Phi\left(\hat{r}_{s,ref},\hat{v}_r\right) = \mathrm{Arg}\begin{pmatrix} x_V\left(\hat{r}_{s,ref},\hat{v}_r,1\right) \\ \times x_V\left(\hat{r}_{s,ref},\hat{v}_r,0\right)^* \end{pmatrix} = \frac{2\omega_T}{c}\left(\frac{b}{2}\sin\theta\right)$$

For any particular pixel in the range-velocity map

$$\begin{aligned} v_s &= \hat{v}_r + v_a\sin\theta \\ &= \hat{v}_r + v_a\frac{c}{b\omega_T}\Phi\left(\hat{r}_{s,ref},\hat{v}_r\right) \end{aligned}$$

All parameters known or calculated

As with all interferometers, the residual noise in the range-velocity maps will lend an uncertainty to the precision of the target velocity measure.

So, for every pixel in the range-velocity map we may estimate the pixel's velocity due to target motion. Where a moving target exists, this will be non-zero.

Our problem then becomes one of detecting whether a significant velocity change (from zero) exists in the presence of noise.

130

130

Along Track Interferometry (ATI)

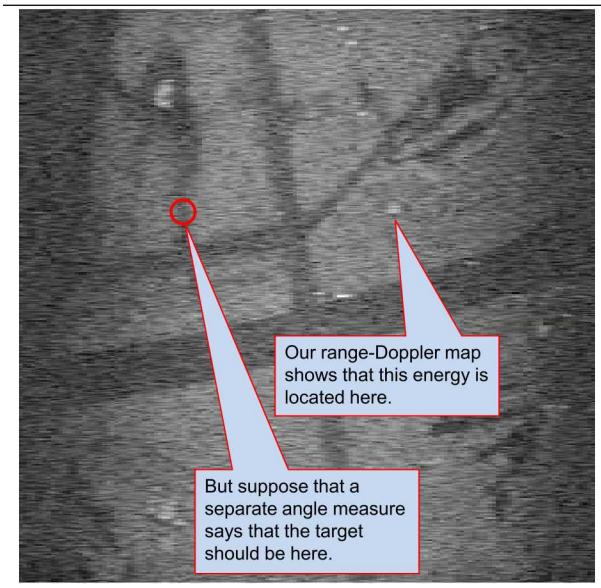

Alternatively, suppose that we had a separate angle measure for each and every pixel in a range-Doppler map.

If the separate angle measure shows the direction of the echo is different than to where it shows up in the range-Doppler map, then the target's energy must have been shifted due to its motion.

So this pixel's echo energy must be from a slow mover.

131

131

Processing – ATI

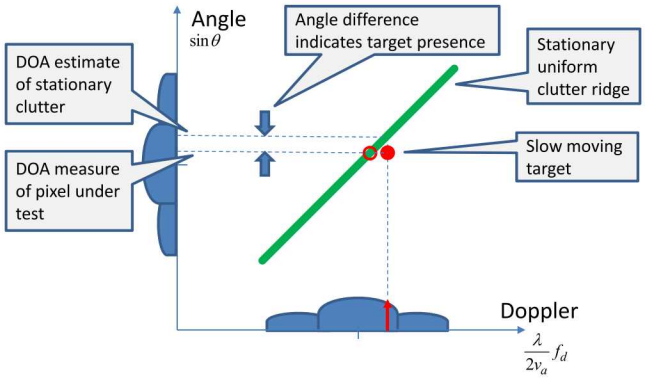

132

132

Processing – STAP (Space-Time Adaptive Processing)

STAP is about processing across multiple antenna phase centers to adaptively null out stationary clutter (and other interfering energy).

This is accomplished by adjusting the overall antenna beam to drive the clutter response (and other interfering energy) into the noise level. A common technique for doing so uses the method of Lagrange multipliers.

The "adaptation" part is about parameterizing this filter to local clutter and noise statistics, which are measured in the echo data.

133

133

Processing – STAP

For each and every range-velocity combination, we want to examine the data over the physical antenna array to see if a signal can be detected in the presence of noise and whatever interference/clutter may exist.

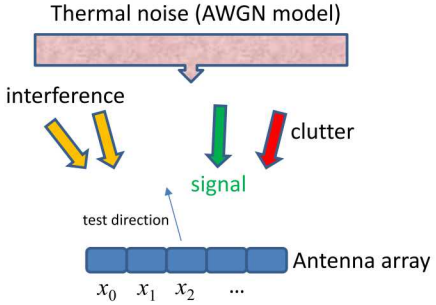

We wish our filter to 'adapt' to the RF environment, to maximize our ability to detect the signal, with minimum expected mean-squared-error.

$\mathbf{w}_{opt} = \left(\mathbf{v}_s^H \mathbf{R}_{\mathbf{nn}}^{-1} \mathbf{v}_s\right)^{-1} \mathbf{R}_{\mathbf{nn}}^{-1} \mathbf{v}_s =$ optimal weights

where $\mathbf{R}_{\mathbf{nn}} =$ Covariance matrix of everything undesired

$\mathbf{v}_s =$ Steering vector for desired look direction

$y = \mathbf{w}_{opt}^H \mathbf{x} =$ Optimally filtered output

"Adaptive beamforming"

134

134

Processing – STAP

The performance of STAP is highly dependent on accurate estimation of the covariance matrix

$\mathbf{R_{nn}}$ — Hard part

This is especially difficult due to

1. Limited data with which to estimate
2. Nonhomogeneous clutter from which to estimate

These difficulties lead to suboptimal filters, which lead to excessive false alarms and reduced detection probabilities.

Schemes to deal with these difficulties abound.

More recently, there has been some success in developing the optimal filter without overtly calculating the covariance matrix, usually involving some iterative adaptation.

As with DPCA, the nulls generated have non-zero width, and targets with slow velocities will still be still be attenuated.

This attenuation is sometimes called "STAP loss."

Null width, and hence MDV, is more a function of antenna total size than the number of phase centers.

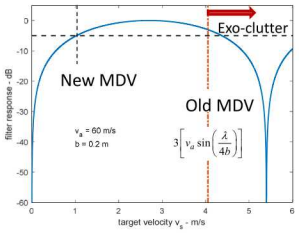

135

135

Processing – STAP

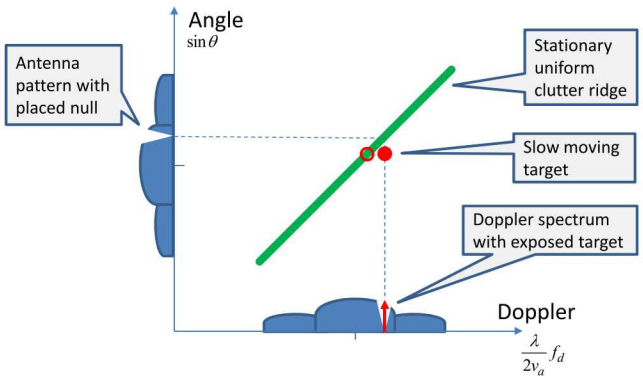

136

136

Processing Comments

- **All algorithms have many variations**
- **Previous analysis was all done with displaced phase center antennas (i.e. phase monopulse)**
  - **Could also be achieved with amplitude monopulse architecture**
- **DPCA and ATI analysis presumed two phase centers**
  - **Can also use more than two phase centers to some advantage**
- **Previous analysis assumed phase centers aligned with flight path**
  - **Can also work with phase centers 'not' aligned with flight path,**
    - but processing gets a little more complicated
- **Clutter notches have some non-zero width**
  - **Depend on overall width of whole antenna**
  - **Will also attenuate slow-moving real targets**
- **Bigger antennas always better**
  - **With respect to narrower clutter notches**
    - Allowing lower MDV

137

137

Processing Comments – Noise Equivalent RCS

GMTI Processing:

Begin with an average +10 dBsm vehicle target RCS
Subtract 10 dB because we want to detect 10th percentile target
Subtract 5 dB of STAP loss
Subtract a minimum 15 dB SNR for detection

Requires Noise equivalent RCS to be at or below –20 dBsm

DMTI Processing:

Begin with an average –10 dBsm 10th percentile target RCS
Subtract 5 dB of STAP loss
Subtract a minimum 15 dB SNR for detection

Requires Noise equivalent RCS to be at or below –30 dBsm

138

138

Processing Comments

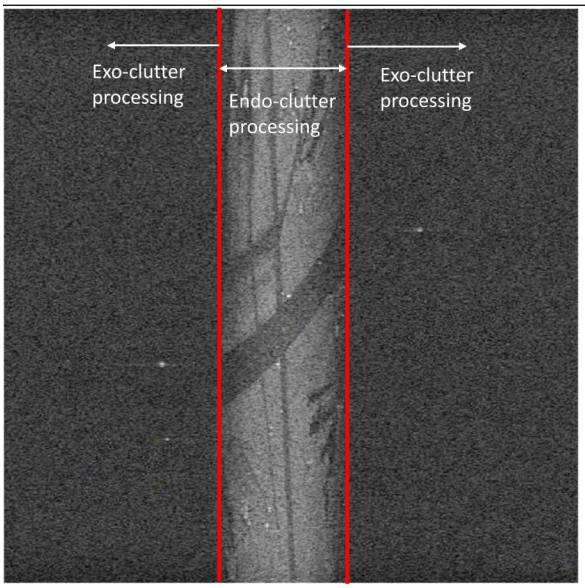

While the various multi-channel processing algorithms are effective in the endo-clutter region,

exo-clutter target detection can remain as for simple single-channel processing.

139

139

Moving Target Geolocation

Courtesy Wikimedia.org

Clearly, we desire to know accurately just where the moving targets are located; placing them in their correct location, and on their correct path.

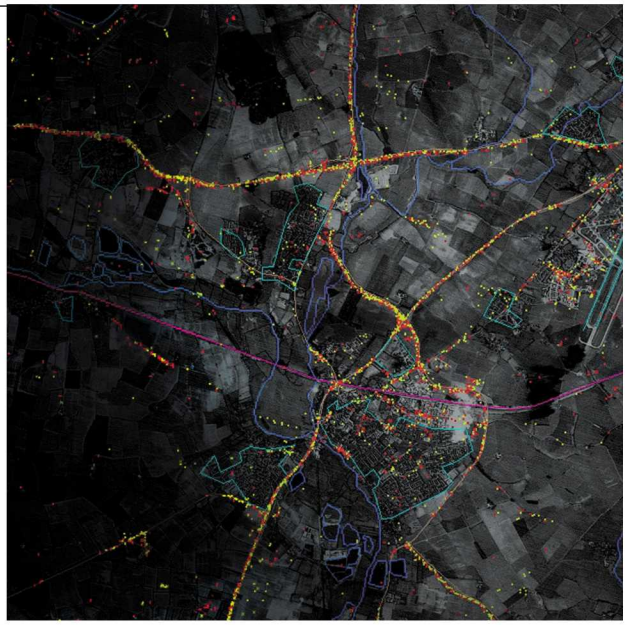

140

140

Moving Target Geolocation

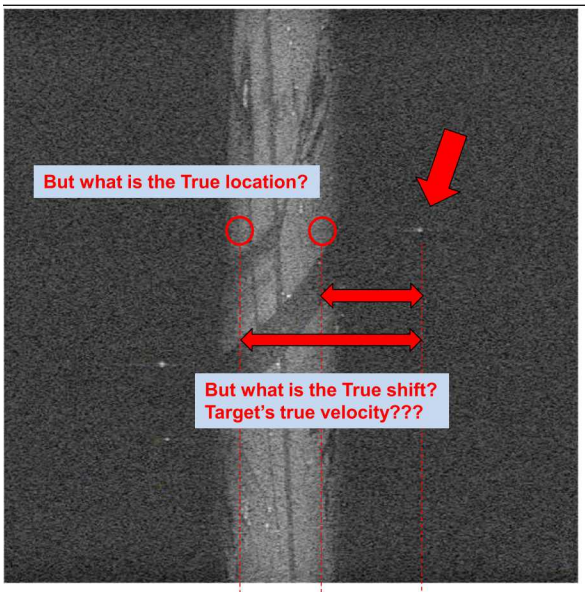

Actually, multiple antenna beams allows separating position information from velocity information.

We can now resolve this ambiguity as well.

Consequently, multiple antenna beams allow more accurate azimuth position information.

Two or more antennas allow improved exo-clutter Direction of Arrival (DOA) measurement.

141

141

How many antenna beams are enough?

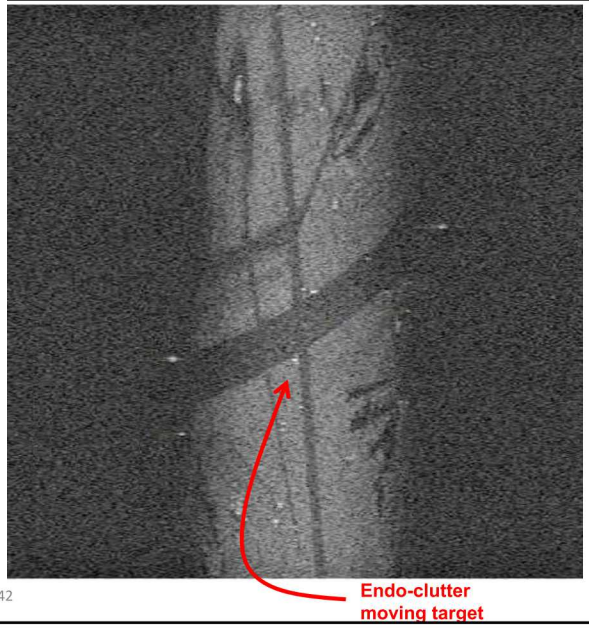

For moving vehicles within the clutter band, any one pixel is a sum of both moving target energy, and stationary clutter energy.

This messes up the DOA measurement. While two antenna beams allows detection inside the clutter, target location is still inaccurate inside the clutter.

To facilitate good moving target location accuracy inside the clutter, we need three or more antenna phase centers (beams)

142

142

How many antenna beams are enough?

Fundamentally, N samples can produce N-1 independent nulls.

In addition, we can view the problem of determining DOA as one of optimal null-steering.

Courtesy GlobalSecurity.org

J-STARS – 3 phase centers

Photo by Alan Radecki

NGC VADER – 4 phase centers

143

One phase center can "detect" an exo-clutter target,
but does a poor job of DOA; limits DOA to "within the antenna beam."

Two phase centers allow "detecting" an endo-clutter target,
but DOA estimation for a single exo-clutter target.

Three phase centers allow DOA estimation for an endo-clutter target.

Additional phase centers allow nulling additional interfering signals; one additional interfering signal for each additional phase center.

Phase centers are assumed to be linear in azimuth

143

Processing Comments – Clutter Notch and MDV

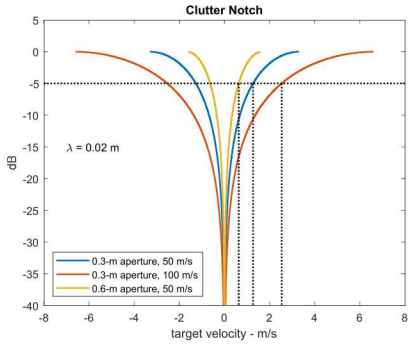

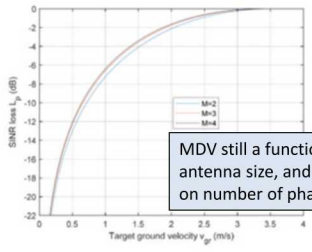

MDV still a function of overall antenna size, and not so much on number of phase centers.

144

The topic of MDV for clutter-cancelling systems is somewhat complicated.

Finite sizes of antennas mean that as target velocity goes to zero, attenuation falls off continuously.

This means that in addition to antenna beamwidth and radar velocity, detectability depends on how much attenuation can be tolerated for a specific target. The MDV depends on how "bright" the target RCS is, along with its velocity.

A "rule-of-thumb" has emerged that declares the MDV as the velocity where attenuation equals 5 dB. In the range-Doppler map this brings the MDV to about 1/3 of the -3 dB beamwidth.

Sometimes called "STAP losses."

144

Processing – Clutter Discretes

What is this?
- Moving Target?
- Bright Stationary target in antenna sidelobe?
- Spurious Response?

Recall that not every possible detection is a real target.

Suppose we wish to detect dismounts with RCS as low as -10 dBsm.

Now suppose that we have a clutter discrete at +45 dBsm that manifests at the same range-velocity position.

This means we have to suppress the clutter discrete by 55 dB to make it appear as dimmer than a real dismount target.

145

145

Processing – Clutter Discretes

Consider a uniformly-illuminated aperture, with two-way antenna response as follows.

Note that outside of the mainlobe, the first six sidelobes attenuate clutter by less than the required 55 dB.

Our endo-clutter processing techniques are meant to operate in the mainlobe only, where we have significant distributed clutter.

Sidelobe targets are more of an exo-clutter issue.

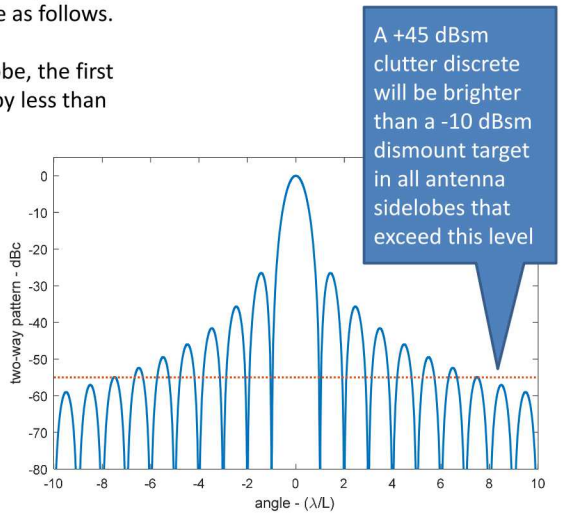

146

146

Processing – Clutter Discretes

Tapering the antenna aperture on some combination of TX and RX beams can substantially lower sidelobe responses.

However, at the same time it affects the nature of any subaperture responses by shifting phase centers and affecting their relative gains.

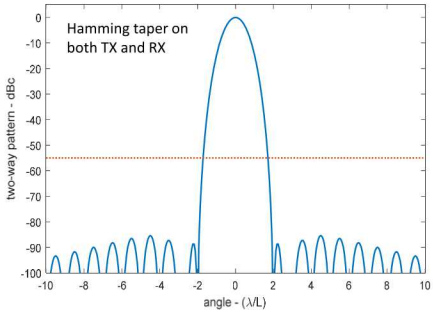

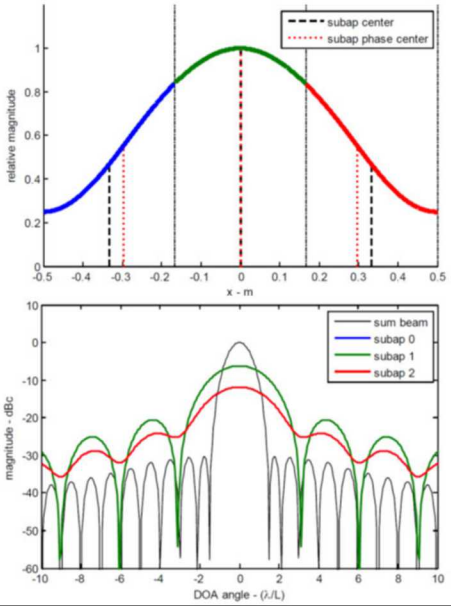

147

147

Processing – Clutter Discretes

An alternative is to employ a second antenna with much broader beam and compare responses as a function of angles. Any responses stronger in the broader "guard" channel must be from a sidelobe echo, and can therefore be ignored, or "blanked."

With a little more processing it can in fact be adaptively "cancelled," if so desired.

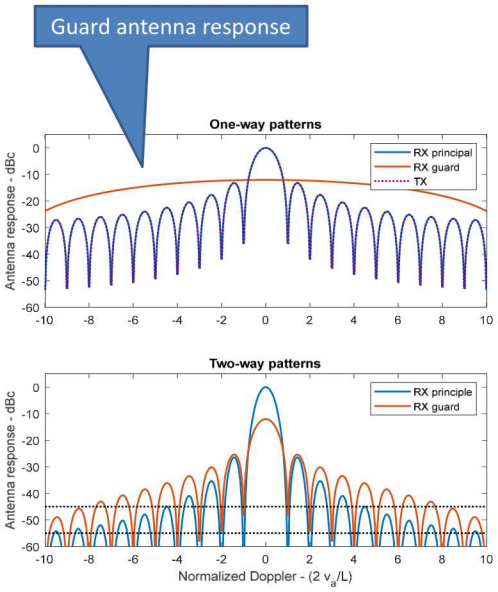

148

148

Processing – Clutter Discretes

In some cases, a monopulse difference channel might serve as a guard channel.

All that is required is a guard antenna response that is stronger than that of the primary antenna in the region of its sidelobes.

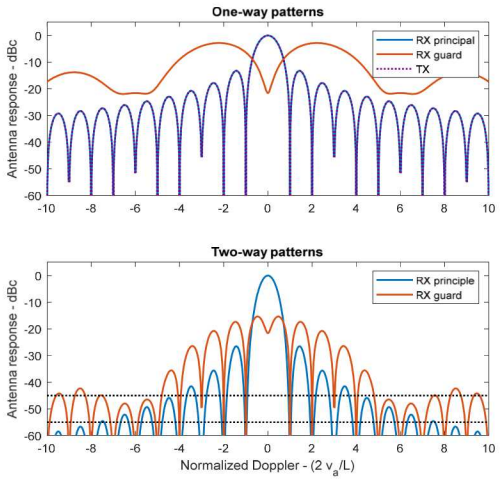

149

Processing – Clutter Discretes

In addition, other techniques might be employed to discriminate between legitimate moving targets and problematic clutter discretes.

These might include:

- Scan-to-scan processing
- Target tracking
- Micro-Doppler analysis
- High-Range-Resolution signature analysis
- Contextual information (road networks, etc.)
- Radar shadow analysis

150

Processing – Other Interferences

Other phenomena might also pose as false targets, and may need careful design choices and mitigation techniques. These might include

ADC nonlinearities
I/Q balance
Jamming/spoofing resistance

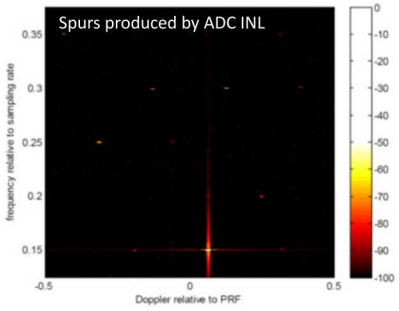

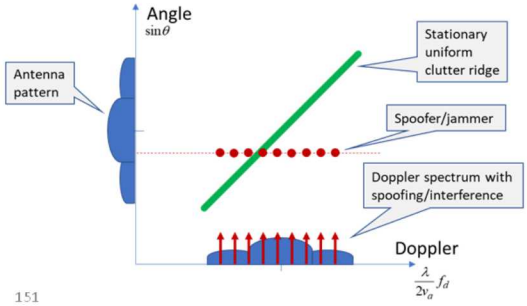

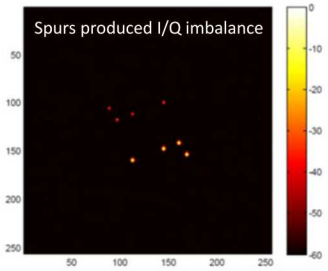

151

151

Section Summary

- **The challenge for GMTI and DMTI radar operation is dealing with clutter.**
- **Clutter may be distributed and/or discrete**
- **All multi-channel (multi-phase-center, multi-beam) processing algorithms attempt to discriminate moving targets from stationary clutter**
  - **2 phase center allow endo-clutter detection and exo-clutter DOA**
  - **3 phase centers allow endo-clutter DOA**
  - **More phase-centers also allow mitigating jammers**

152

152

Select References

- Clutter in the GMTI Range-Velocity Map
  - Sandia National Laboratories Report SAND2009-1797
- Radar Channel Balancing with Commutation
  - Sandia National Laboratories Report SAND2014-1071
- GMTI Direction of Arrival Measurements from Multiple Phase Centers,
  - Sandia National Laboratories Report SAND2015-2310
- Limits to Clutter Cancellation in Multi-Aperture GMTI Data,
  - Sandia National Laboratories Report SAND2015-2311
- Some comments on performance requirements for DMTI radar
  - SPIE Proceedings Vol. 9077
- Measuring Balance Across Multiple Radar Receiver Channels,
  - Sandia National Laboratories Report SAND2018-3068
- On minimum detectable velocity
  - SPIE 2019 Proceedings Vol. 11003
- Space-Time Adaptive Processing
  - J. R. Guerci, ISBN 1-58053-377-9, Artech House, Inc.
- Clutter Locus for Arbitrary Uniform Linear Array Orientation
  - Sandia National Laboratories Report SAND2010-8796
- Phase Centers of Subapertures in a Tapered Aperture Array
  - Sandia National Laboratories Report SAND2015-9566
- Antenna Requirements for GMTI Radar Systems
  - Sandia National Laboratories Report SAND2020-2378

153

153

GMTI Ancillary Topics

- Monopulse Antennae
- Xpol effects
- HRR
- Tracking
- Variety of moving targets
- Vibrometry
- Micro-Doppler
- VideoSAR – shadow tracking
- VideoCCD

154

154

Monopulse Antenna

IEEE Standard 145-1983 defines "monopulse" as

> "Simultaneous lobing whereby direction-finding information is obtainable from a single pulse."

No specific mention is made of number of antenna beams or phase centers.

More colloquially, only two beams or phase centers are assumed in any baseline orientation.

Furthermore, "lobes" are often combined into "sum" and "difference" channels, by microwave circuits known as "monopulse networks," "hybrids," "magic-T networks," and other terms.

Not specifically necessary to be a monopulse antenna system

155

155

Monopulse Antenna

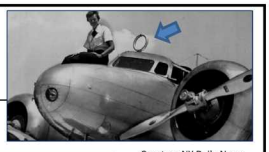

Courtesy NY Daily News

Monopulse techniques are derived from early tracking radars, where the ratio of separate beams were used directly to drive the pointing of an antenna to keep it centered onto a target.

"Monopulse" refers to the ability to determine Direction of Arrival (DOA) using "nulls" generated from multiple beams with a single pulse.

Courtesy BAE Systems

An inherent truth with filters and antenna beams is that "nulls" are much sharper (more localized) than peaks.

-- better suited for DOA measurements

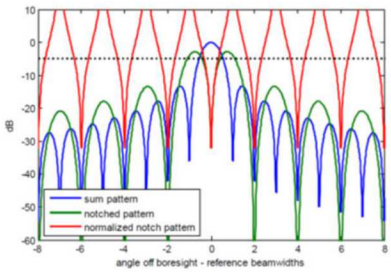

Uniformly illuminated aperture

- blue = sum pattern
- green = left – right

156

156

Monopulse Antenna

Two main classes of Monopulse antennae

Phase Monopulse antennae generate multiple beams from separate phase centers, but beams are typically pointed in the same direction. DOA is calculated via interferometry.

Amplitude Monopulse antennae generate multiple beams from the same phase center, but beams are typically pointed in offset directions. DOA is calculated via comparing beam strength.

Hybrid systems also exist

The choice between amplitude versus phase monopulse is more about convenience for a particular antenna technology (e.g. dish vs. flat panel array). Otherwise there is no real advantage of one over the other for a given antenna size constraint.

157

157

How to measure angle: **Phase Monopulse Antenna**

In this configuration, we have two beams with slightly different phase center locations, but otherwise squinted the same.

Each beam has slightly different range to target, manifesting as a slight phase-difference in the respective target echoes.

The phase difference depends on how left or right the target is with respect to the boresight direction.

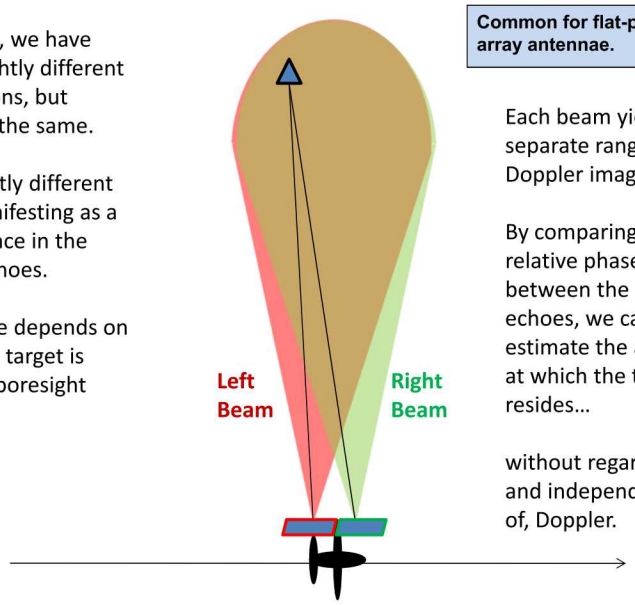

Common for flat-panel array antennae.

Each beam yields a separate range-Doppler image.

By comparing the relative phase between the echoes, we can estimate the angle at which the target resides…

without regard for, and independent of, Doppler.

158

158

How to measure angle: **Amplitude Monopulse Antenna**

In this configuration, we have two beams slightly squinted with respect to each other.

Each beam has angle-dependent gain, but since the beams have different squint, their angle-dependent gains are different from each other.

Target direction A has more gain in the left beam than the right beam.

Target direction B has equal gains in both beams.

Target direction C has more gain in the right beam than the left beam.

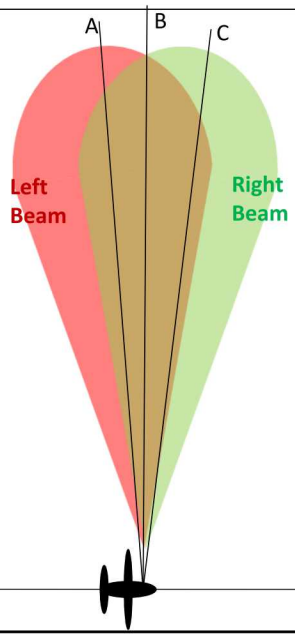

Common for dish reflector antennae.

Each beam yields a separate range-Doppler image.

By comparing the relative strength of target echo in both images, we can estimate the angle at which the target resides…

without regard for, and independent of, Doppler.

159

159

Amplitude Monopulse Antenna

Dual-Feed Reflector Antenna

By using two feeds, each slightly offset from the focal point of a reflector antenna, we can create the two beams with effectively common origin, but slightly different squint angles.

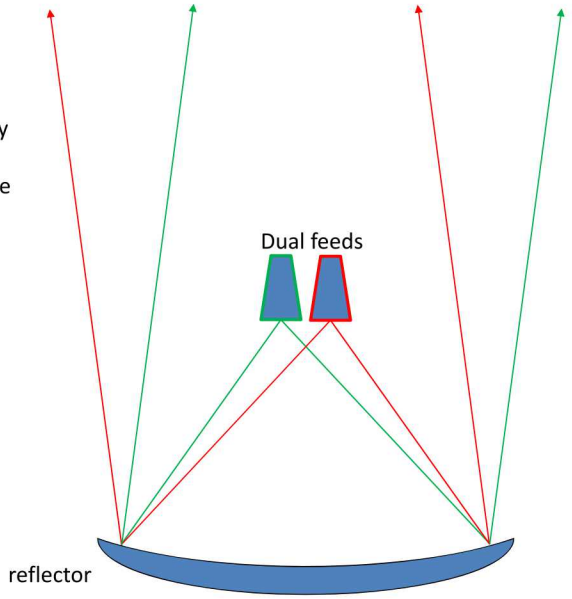

160

160

Amplitude Monopulse Antenna

For signal processing convenience, frequently instead of left and right channels, the radar receives sum and difference channels.

The monopulse network is bi-directional.

The transmitted signal is usually fed to the sum channel, so that it is applied equally to both feeds,

Has some advantages when dealing with processing channel imbalances.

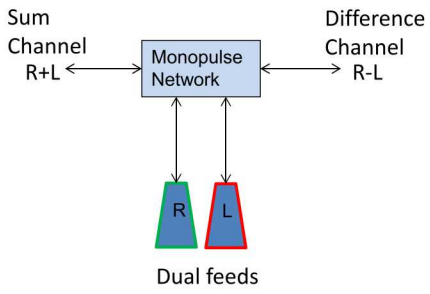

161

161

Cross-Polarization Echo

Consider an antenna aperture conformal to a spherical surface.

Note that a linear polarization is rotated in a manner dependent on the local position on the curved surface.

This means that a difference between left and right sides of the RX antenna will depend on the polarization of the returned echo signal.

Any null for, say, a desired V signal will contain energy from the undesired cross-pol H signal.

-- fills in the null
-- reduces clutter cancellation
-- sensitive to cross-pol jammers

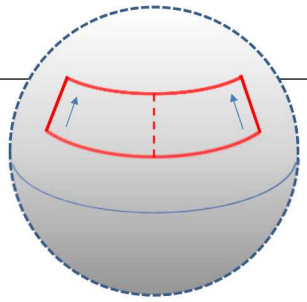

True for any aperture on a curved surface

-- conformal arrays
-- parabolic reflectors

May need mitigation schemes

162

162

Cross-Polarization Echo

Example:

Consider clutter with a relative cross-pol response of -6 dB compared to a co-pol response.

Now consider an antenna with only 15 dB of cross-pol rejection.

This means that the clutter suppression in the center of a null is limited to 21 dB, which is pretty poor.

Mitigation steps include

1. Avoiding curved apertures
2. using polarization-sensitive screens and reflectors
3. Collecting and processing fully polarimetric data

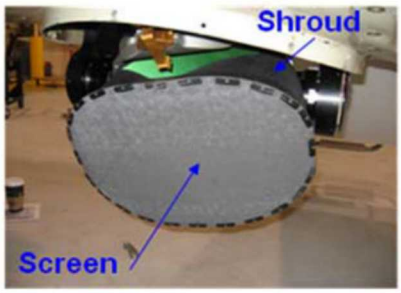

163

163

High-Range-Resolution (HRR) GMTI

Fine range-resolution allows High-Range-Resolution (HRR) GMTI.

This allows exploiting vehicles' unique range profiles for moving target discrimination and perhaps even identification.

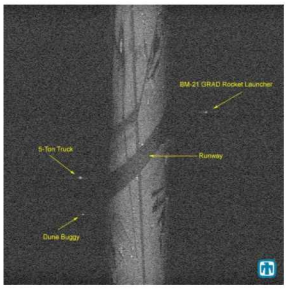

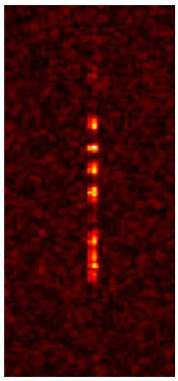

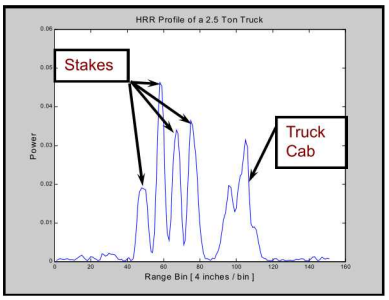

164

164

Target Tracking

It is often not sufficient to know the location of all moving targets.

In particular, we often want to follow a *particular* moving target, i.e. keep custody of it,

or understand from where, and/or to where, those targets are moving, i.e. a *time-history*.

This means 'tracking' those targets.

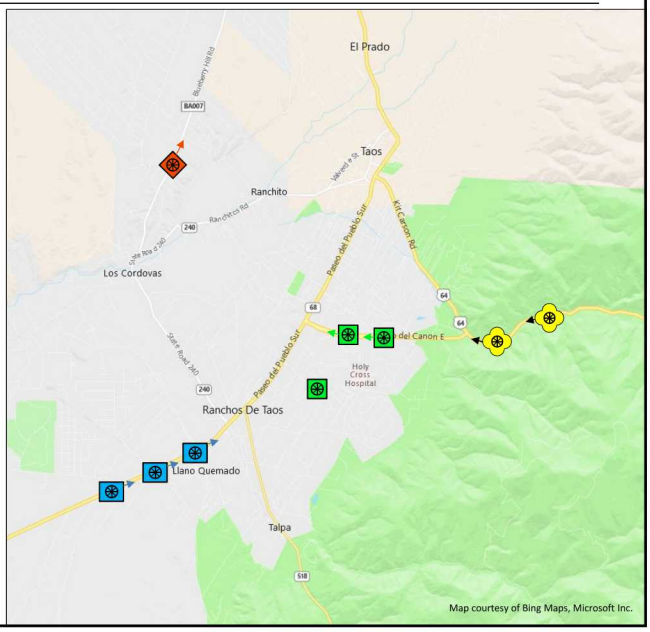

165

165

Target Tracking

One application of GMTI tracks is sometimes called "Forensic" GMTI;

Assessing the travel history of a moving target.

This makes it advantageous to record, store, and archive GMTI data.

(Also useful for Pattern-of-Life analysis.)

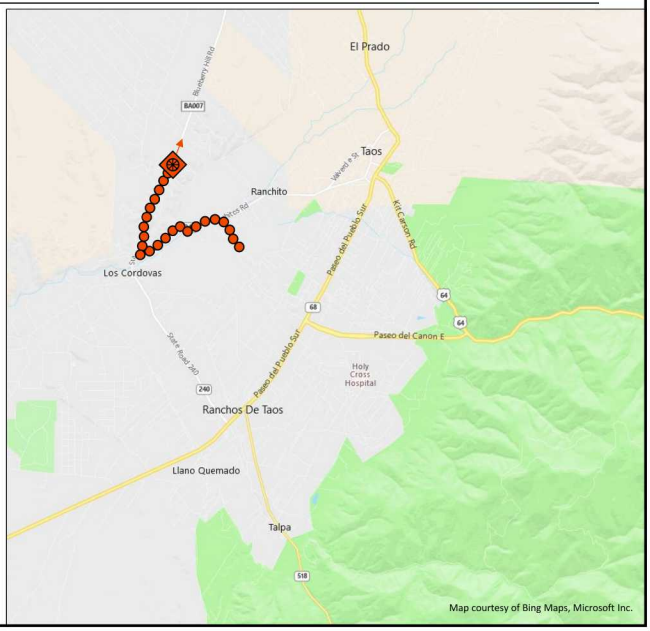

166

166

Moving Features – Translation

167

167

Moving Features – Rotation

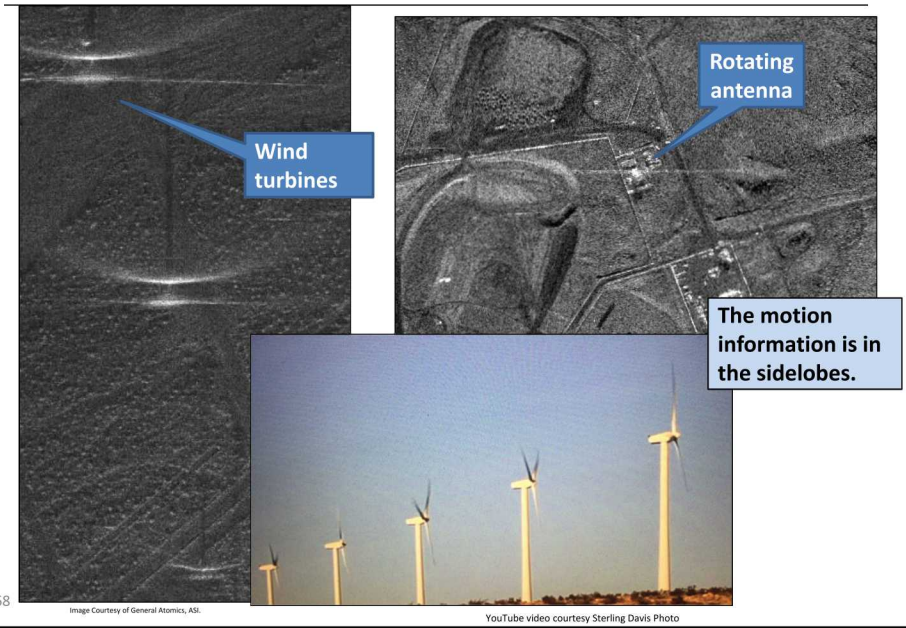

168

Image Courtesy of General Atomics, ASI.

YouTube video courtesy Sterling Davis Photo

168

Moving Features – Vibration

Vibration and rotation involve alternating positive and negative line-of-sight velocities during a synthetic aperture.

These will tend to throw Doppler sidelobes in both directions.

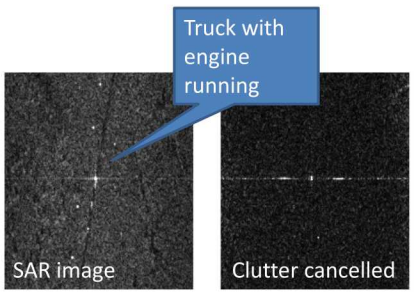

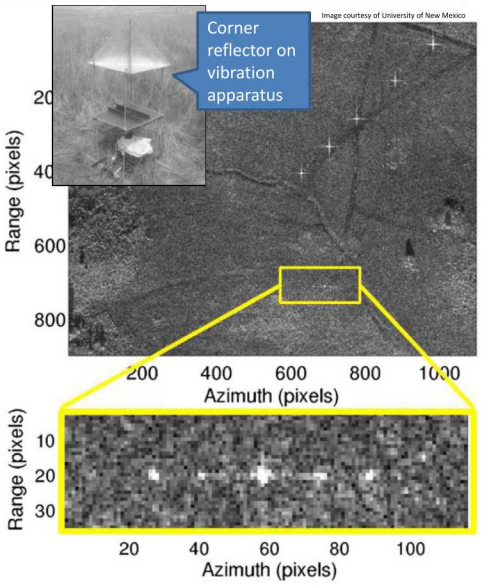

169

169

Moving Features – Vibration

170

170

Moving Features – People

People generally can't hold still enough to focus well. They tend to smear in Doppler even when standing still. However, their shadows don't exhibit Doppler effects.

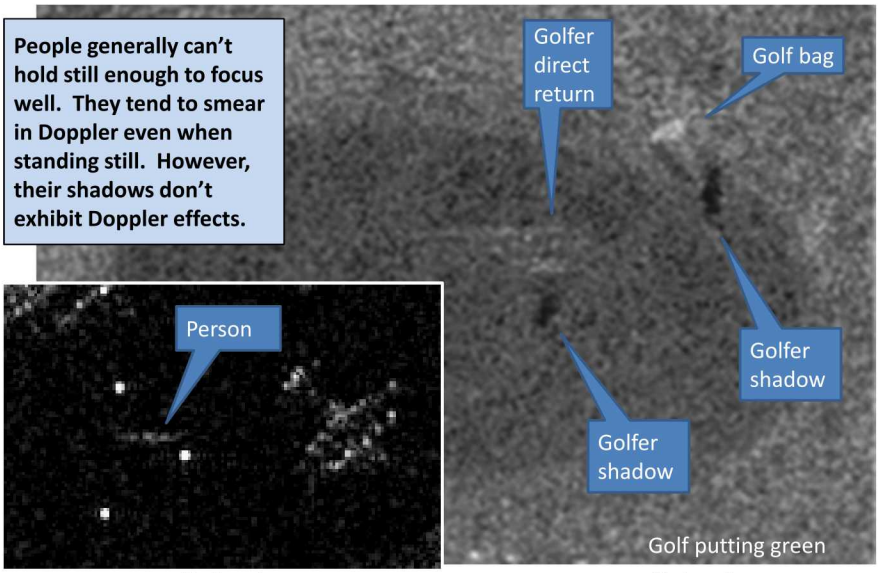

171 Ku-band Ka-band

171

Moving Features – Blowing Trees

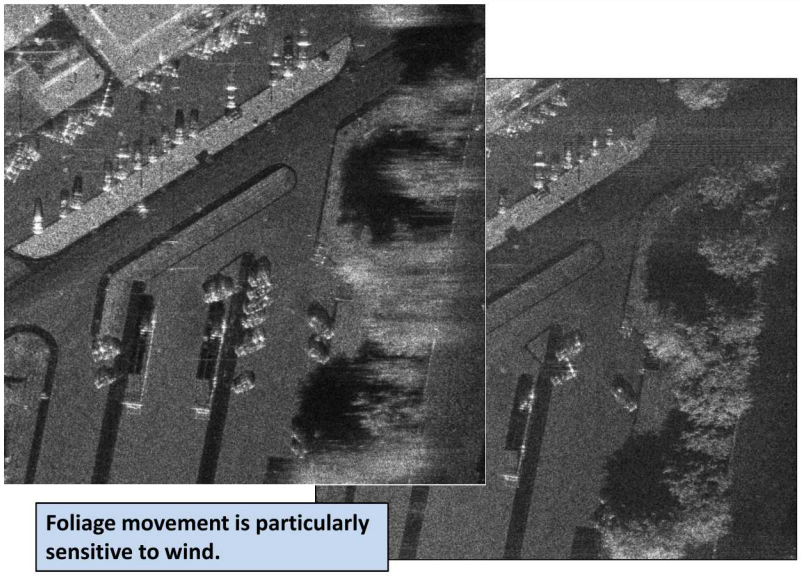

Foliage movement is particularly sensitive to wind.

172

172

Micro-Doppler

Most moving targets are assumed to be rigid bodies for purposes of detection, or at least dominated by a principal scattering center that is fairly rigid.

However, most moving targets are *not* strictly rigid, with components that exhibit different motion than the principal scattering center, e.g. wheels, tracks, articulated limbs, etc.

These secondary scattering centers with different motion are often observable and resolvable with different Doppler signatures, i.e. Micro-Doppler.

They can be used to characterize, and perhaps to discriminate targets.

173

173

MicroDoppler – Vehicle Signatures

Full UHRR Range/Doppler Image

Photograph of 2.5 Ton Truck

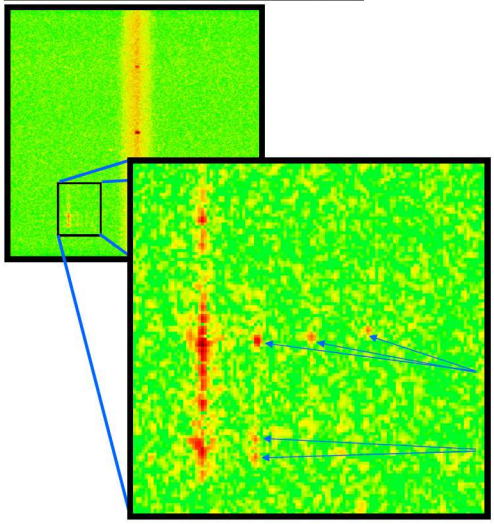

Radar returns from front axle lug nuts

Radar returns from dual rear axles

UHRR Signature of 2.5 Ton Truck (4 inch range resolution)

174

174

Micro-Doppler – Motion Analysis

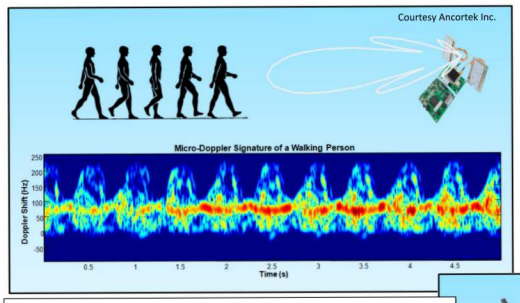

Micro-Doppler analysis allows assessment of articulated motion, leading to classification and identification of target classes, activities, and state-of-health.

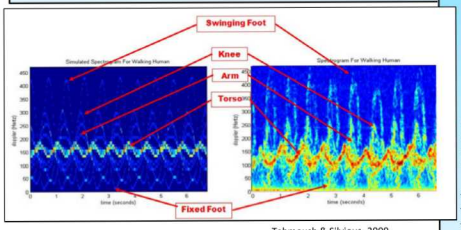

Tahmoush & Silvious, 2009

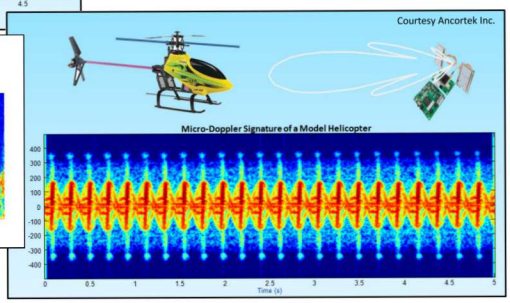

175

175

VideoSAR

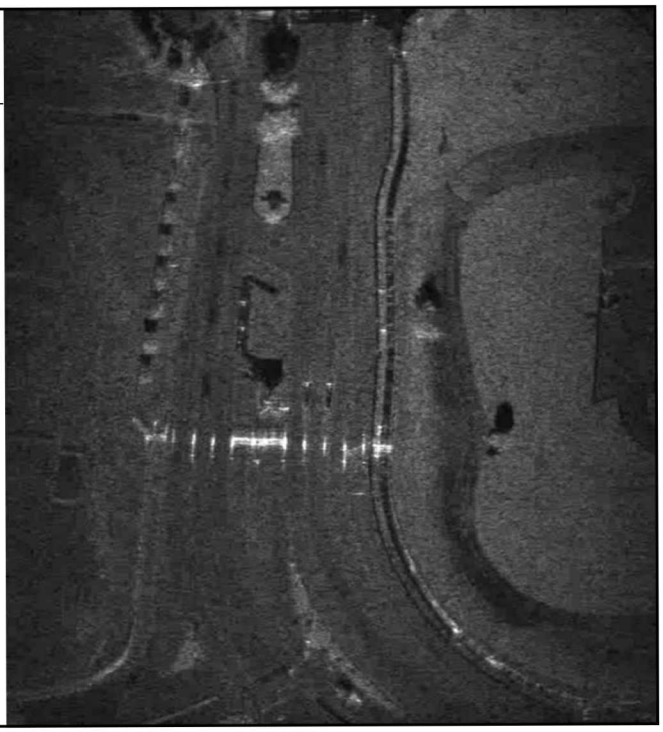

176

176

Human-Machine-Interface (HMI) and Workflows

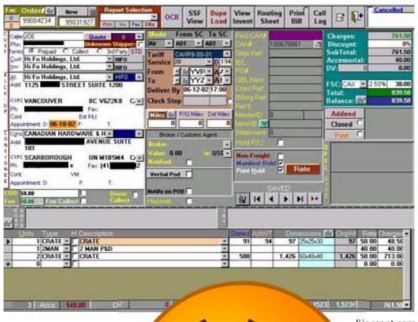

blogspot.com

Not so good

Wikimedia

With ever more complex tasks being performed by ever fewer crew, it is essential that sensor interfaces be easy and intuitive.

Many multi-sensor systems do *not* have a dedicated radar operator

Airman 1st Class Michael Shoemaker/USAF/Reuters

177

177

Section Summary

- **Multi-aperture, multi-beam antennas are generically referred to as Monopulse antennas**
  - **Regardless of number of phase-centers or beams**
  - **Two types; "Amplitude" and "Phase" monopulse**
- **The utility of GMTI/DMTI is considerably enhanced by employing Target Tracking capability**
- **Micro-Doppler is the Doppler variations due to a target not being entirely a rigid body**
- **Target motion can also be detected and measured from the movement of radar shadows in a sequence of SAR images**

178

178

Select References

- Monopulse Principles and Techniques – second edition
  - Samuel M. Sherman & David K. Barton, ISBN 160807174X, Artech House, Inc.
- Apodization of Spurs in Radar Receivers Using Multi-Channel Processing,
  - Sandia National Laboratories Report SAND2014-1678
- Performance effect of unintended polarization on clutter attenuation
  - SPIE 2019 Proceedings Vol. 11003
- A crash course in basic single-scan target tracking (abridged)
  - SPIE 2018 Proceedings Vol. 10633
- Stationary and moving target shadow characteristics in synthetic aperture radar
  - SPIE 2014 Proceedings Vol. 9077
- Impact of Ground Mover Motion and Windowing on Stationary and Moving Shadows in Synthetic Aperture Radar Imagery
  - SPIE 2015 Proceedings Vol. 9475

179

179

The End

www.doerry.us

Christian Hülsmeyer

180

180